THE COLLECTION OF UNIFORM LATEX AEROSOL PARTICLES BY CHARGED WATER DROPLETS

A THESIS

Presented to

The Faculty of the Division

of Graduate Studies

By

Ronald Dennis

In Partial Fulfillment

of the Requirements for the Degree

Master of Science in the School

of Chemical Engineering

Georgia Institute of Technology

August, 1975

THE COLLECTION OF UNIFORM LATEX AEROSOL PARTICLES BY CHARGED WATER DROPLETS

Approved:

Michael J. Matteson, Chairman

Clyde Orr, Jr.

Henderson C. Ward

Date approved by Chairman: 8-19-75

ACKNOWLEDGMENTS

I would like to express my appreciation to my thesis advisor, Dr. Michael J. Matteson, for his direction and encouragement. I would also like to thank Dr. Clyde Orr, Jr. for his time and very helpful advice.

Finally, I would like to thank the members of Aunt Frances's Wednesday night Bible study group for their prayers and encouragement.

TABLE OF CONTENTS

LIST OF TABLES

LIST OF ILLUSTRATIONS

Figure Page

SUMMARY

The collection of uniform latex aerosol particles by charged water droplets was studied. The aerosol was generated from an aqueous solution of uniform latex particles containing 10% solids by weight. The water droplets were charged by passing distilled water through a No. 26 hypodermic needle which was attached to a constant voltage source. The water droplets were formed in a chamber filled with aerosol which allowed the collection of the particles on the droplet only during the formation period. As soon as the droplet was formed, it fell through a flushing air chamber fitted with a grounded steel base. The collected water was withdrawn and analyzed for latex by a spectrophotometer. By measuring the surface area and charge, the amount of aerosol collected per droplet was correlated with the surface charge density. It was found that in most cases there was an increase in collection efficiency with surface charge density; however, after a certain amount of surface charge density, no further changes in collection efficiency were noted.

CHAPTER I

INTRODUCTION

Since passage of the Clean Air Act of 1970, air pollution in the United States has received more and more attention. Parallel with this intensive interest in the problem of air pollution, is the continued emission of greater and greater amounts of air pollutants into the atmosphere. To halt this growing menace, various federal and state agencies were established with large amounts of federal and state funds. To date, these agencies have contributed significantly to the alleviation of air pollution; however, the air pollution menance marches on.

Every year more and more sulfur dioxide, oxides of nitrogen, carbon monoxide, and particulates enter the atmosphere from existing and new emission sources. These pollutants increase because efficient methods for removing them have not been discovered. Much work has been done on the removal of sulfur and nitrogen from stack gases; however, most of the work done on the removal of particulates from these gases has been in the relatively expensive but efficient method of electrostatic precipitation.

Wet scrubbing is a fairly efficient, relatively inexpensive anti-pollution system in wide use today. This

process involves bringing a liquid, usually water, into contact with the stack gas and absorbing the noxious gases in the liquid. In most applications of wet scrubbing, only the removal of noxious gases from the stack has been considered. Very little consideration has been given to the use of this method for the removal of particulates from gas streams.

Much work has been done investigating the collection of aerosol particles. Fuchs [1], Davies [2], and Green and Lane [3] have produced several good reviews on the subject. Wilson [4], Davies [5], and Fuchs and colleagues [6] have investigated the collection of aerosol particles on the inside walls of tubes and plain surfaces. Zebel [7] and Natanson [8] have contributed in the area of deposition on cylindrical objects which is applicable to filtration.

The collection of dust particles was investigated by Walton and Woolcock [9] and the collection of salt particles by water sprays was investigated by Picknett [10]. The collection of an aqueous mist of water drops being formed on glass beads was examined by Khimach and Shishkin [11]. A theory was proposed by Pemberton [12] for calculating the scavenging effects of rain on particulate matter suspended in the air. This theory was later tested by Oakes [13]. In addition, Fonda and Herne [14] proposed a workable theory for the deposition of aerosols on spheres and Lundgren and Whitby [15] developed an empirical equation for this phenomena.

Little of the work mentioned above dealt with charged spheres and none considered charged liquid spheres; however, there has been significant research in this area. Gillespie [16] reviewed electrical charge effects in aerosol particle collision phenomena; the last study of which considered charged liquid spheres. This study was done by Gunn and Hitschfeld [17].

Gunn and Hitschfeld showed experimentally that the collection efficiency of a 1 mm drop falling through a cloud of droplets (mean diameter 1 μ) is not effected by charging the droplet electrically to 2 e.s.u. This charge was comparable to the charge observed on raindrops in thunderstorms.

On the other hand, a study by Kraemer and Johnstone [18] showed a definite effect of electric charge on spheres on the collection efficiency of aerosol particles. In this study, a LaMer-Sinclair generator was utilized to produce a dioctyl phthalate aerosol. Three different sizes of metal collecting spheres were used--1/4, 3/8, and 7/16 inch in diameter. The aerosol was transported through a collecting cell for a timed period and permitted to deposit on the collecting sphere or to flow out the exhaust hood. At the end of the timed period, the cell was swept clear of aerosol by a metered flow of air. The sphere was next removed from the cell and washed with ethyl alcohol. Ultraviolet absorption was used to analyze the alcohol solution

for dioctyl phthalate. The aerosols used had diameters ranging from 0.54 to 1.18 μm, concentrations ranging from 3.3 to 197 mg/1, and aerosol velocities ranging from 1.56 to 6.89 cm/sec.

Since low flow rates were used in Kraemer and Johnstone's experiments, a parabolic velocity profile prevailed in the collection cell. The following equation was used to calculate the collection efficiency:

$$E = (R_c/R)^2 \times (1-(\frac{w-w_c}{w})^{1/2}) \qquad (1)$$

where

R_c = radius of the collection cell

R = radius of the sphere

w = mass flow rate of aerosol past the collector

w_c = rate of aerosol deposition on the collector

For both charged and uncharged collecting spheres, measurements of E were made. The collection efficiency of aerosols for potential and viscous flows past a conducting sphere due to the electrostatic forces was calculated with the help of a computer. Interception allowances were made but inertial effects were neglected. The ratio of the electric force acting upon a particle located near the surface of the sphere to the quantity $6\pi NrU_o$ was expressed by different dimensionless parameters, K_I. Assuming the validity of Stokes' Law,

the quantity $6\pi NrU_o$ characterizes the resistance of the medium to the motion of the particle. In addition, determinations of the approximate relationships between the various parameters and the collection efficiency were made.

The parameter K_I, derived for induction to a charged sphere and uncharged aerosol, is as follows:

$$K_I = \frac{X_s - 1}{X_s + 2} \frac{4\ Cr^2q^2}{3\varepsilon_o RNU_o} \tag{2}$$

where

q = surface charge density of sphere

r = radius of aerosol particle

R = radius of sphere

X_s = dielectric constant of sphere

ε_o = permittivity of free space

C = Cunningham factor

N = viscosity of medium

U_o = velocity between collecting sphere and aerosol

This equation is based on a physical model of a single collecting sphere surrounded by an infinitude of aerosol particles. It is assumed that the diameter of the collector is much greater than the diameter of the aerosol particle and that the spacing between all bodies, with the possible exception of the collector and one aerosol particle, is much greater than the diameters of the aerosol particles. In

like manner, parameters were given for the following conditions: charged sphere and charged aerosol, K_E; and for charged aerosol and grounded sphere, K_G.

Kraemer and Johnstone calculated the relationship between E and K_I to be as follows:

$$E = ((15/8)\pi K_I)^{0.4} \tag{3}$$

The experimental measurements of collection efficiencies using metal spheres were found to agree quite well with theory.

Matteson and Giardina [19] conducted a study of the absorption of sulfur dioxide by charged water droplets during the formation period. In this study, a given surface charge density was applied to water droplets which were continuously formed at the top of a charged capillary exposed to air containing known concentrations of sulfur dioxide and water vapor. The drops were collected and, by using conductometric techniques, the amount of absorbed sulfur dioxide was determined. This study showed that the rate of mass transfer of SO_2 is increased by applying a surface charge to the water droplet.

Lonzy Lewis [20] investigated the effects of the surface charge density of water droplets on the deposition of a sodium chloride-uranine aerosol. In this study, a

surface charge density was applied to water droplets while being formed at the tip of a charged capillary that was exposed to the sodium chloride-uranine aerosol stream. After the droplet fell from the capillary, contact with the aerosol was terminated and the droplets were collected for a fluorometric analysis.

The collection parameter, K_I, for Lewis's experiments was the same collection parameter determined by Kraemer and Johnstone as previously discussed (see Equation 2).

Lewis's collection efficiency, E, was defined as the ratio of the amount of aerosol collected when the droplet possessed a surface charge, C_a, to the amount collected when there was no surface charge, C_o; therefore, $E = C_a/C_o$ and was equal to unity when no surface charge was present.

Lewis's data for different aerosol flow rates were first plotted as C_a *vs.* q^2. These graphs showed a significant increase in the amount of deposited aerosol with increasing surface charge on the droplets; however, Lewis was unable to determine the exact relationship. In addition, Lewis noted a slight increase in the amount of aerosol deposited when positive voltage was applied compared to when negative voltage was applied.

Using the theory of Kraemer and Johnstone for the relationship between the collection parameter, K_I, and the collection efficiency, E, Lewis plotted graphs for E *vs.* K_I with the experimental data and the theoretical data. These

graphs showed the measured efficiencies to be larger than the theoretical ones in every situation. However, the reason given by Lewis for this deviation was the collection efficiency found in his study was obtained in a manner totally different from the one used by Kraemer and Johnstone. Nevertheless, the slopes of the experimental lines did not differ significantly from those of the theoretical curves; therefore, the theory of Kraemer and Johnstone was found to be a good approximation for the collection efficiencies of aerosol particles on charged liquid spheres.

Pilat, Jaasund, and Sparks [21] made theoretical calculations and conducted experimental measurements showing the collection of small aerosol particles (0.05 to 5 μm diameter) by water droplets in spray scrubbers can be significantly increased by electrostatically charging the droplets and particles to opposite polarities.

Most of the previous work on the mechanism involved in the deposition of aerosol particles on charged water droplets entailed experimentation using polydispersed aerosols. Little work was done on the deposition of monodispersed aerosol particles on charged water droplets. This research was thus designed to investigate the effects of the surface charge density of water droplets on the deposition of various monosized, latex aerosol particles, the effects of different aerosol particle sizes on the deposition at constant flowrates, and the validity of the "Kraemer-Johnstone"

theory derived for the deposition of an uncharged aerosol on a charged sphere.

All of the above objectives were fulfilled by applying a determined surface charge density to water droplets which were continuously being formed at the tip of a charged capillary that was exposed to an aerosol stream. As soon as the droplet fell from the capillary, contact with the aerosol was terminated and the droplets were collected for spectrophotometric analysis.

As previously mentioned, one industrial application of the phenomenon of the deposition of aerosol particles on charged water droplets is wet scrubbing of particulate matter from gas streams. Another application is in the area of atmospheric scavenging of particulate matter. Finally, some applications may be found in inhalation therapy.

CHAPTER II

INSTRUMENTATION AND EQUIPMENT

The equipment for the experiment was required to perform certain specific functions both reliably and accurately. The primary function of the equipment was to generate and charge droplets of water. These droplets then had to be brought into contact with a dry aerosol in such a way that exposure would occur only during the drop formation period. The final function was the collection and analysis of the droplets.

Several additional requirements of importance had to be imposed on the equipment. First, in the generation of the aerosol, a wet stream had to be generated, dried, and properly channeled such that measured amounts would be brought into contact with the water droplets. Another requirement was imposed by virtue of the natural charge of the latex particles. This entailed neutralizing the latex particles by using a radioactive source. Finally, accurate measurements of the drop rate, the charging rate, and all flow rates were required.

The schematic diagram of the experimental apparatus as shown in Figure 1 was composed of several sections according to function.

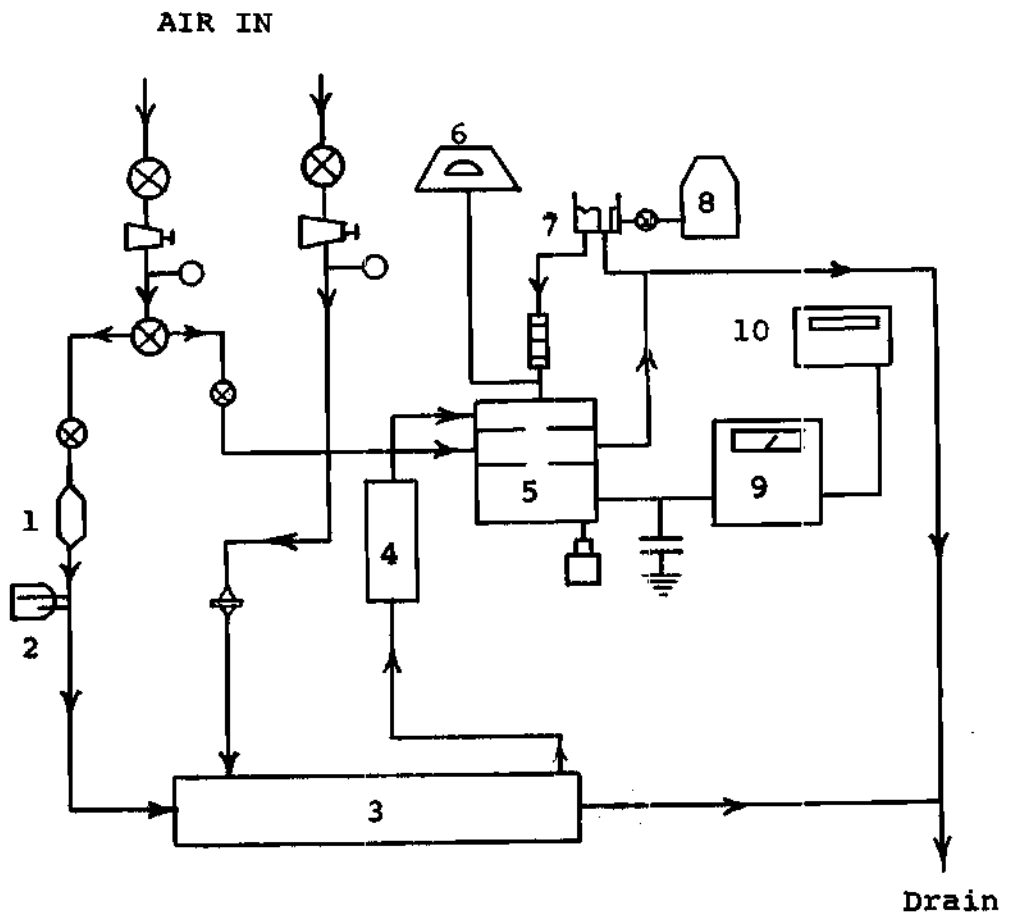

1 Aerosol Generator
2 Collecting Flask
3 Dryer
4 Aerosol Neutralizer
5 Deposition Chamber
6 Voltage Source
7 Constant Head Pressure Regulator
8 H_2O Reservoir
9 Electrometer
10 Digital Voltmeter

Valve
Press. Reg.
Press. Indicator
Millipore Filter
Rotameter
Capacitor

Figure 1. Schematic Diagram of the Experimental Apparatus

The first section contained the necessary equipment to generate and charge the water droplets. This section consisted of a polyethylene reservoir of distilled water, a constant head water pressure regulator, a stopcock, a hypodermic needle, and a high voltage supply. A plexiglass cup served as a pressure regulator by maintaining a constant pressure head of water by means of a drain outlet at a fixed height. The whole assembly could be moved vertically to adjust the flow rate. Distilled water entered the cup by two means. The main exit was through the drain at the center of the cup which ran to the sink. A lesser amount exited through an opening in the bottom of the cup and flowed through the needle to become droplets.

The droplets were produced by allowing water to flow through a No. 26 hypodermic needle which had been ground square and polished at the top. A Beckman high voltage supply, variable from 0 to 25 kv, was connected to the needle to charge the droplets. The high resistance, low pass filter diagrammed in Figure 2 stabilized the voltage supply and protected it against current drain. A Matheson, Model 601, rotameter regulated the flow of the water through the needle.

The second section of the experimental apparatus consisted of the necessary equipment to generate, dry, and neutralize the aerosol. The aerosol generator was a No. 40 DeVilbiss nebulizer which was affixed to one end of the

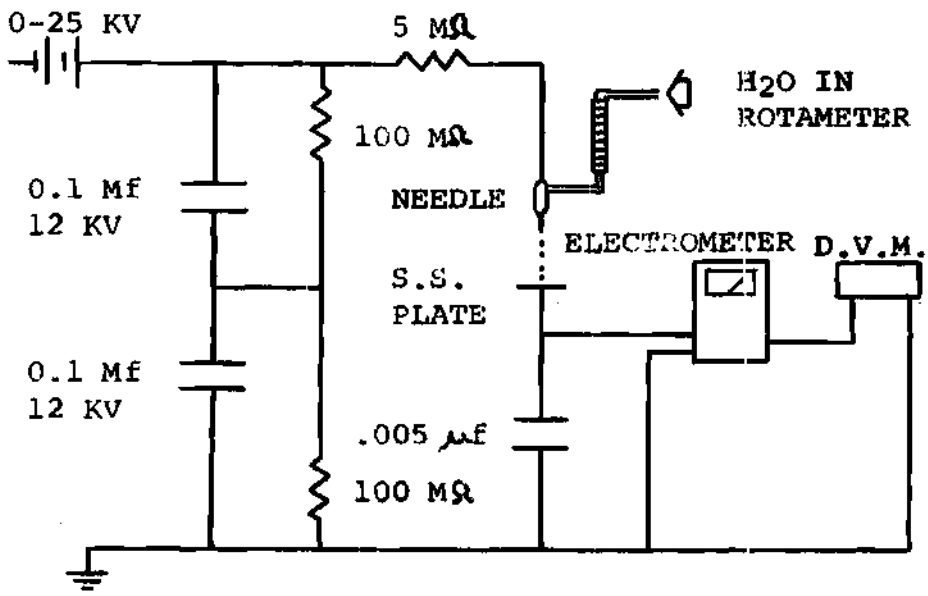

Figure 2. Diagram of the Electrical Apparatus

aerosol dryer (see Figure 3). This dryer was a plexiglass cylinder which was 48 inches long and 2-1/2 inches in diameter. A second supply of dried laboratory air flowed through a millipore filter before entering the dryer from the side near the aerosol generator.

At the end of the dryer, two streams exited. One stream went directly to the drain while the other stream passed through an aerosol neutralizer. This concentric cylinder contained a 2 millicurie radioactive source, Kr-85 gas, which was sealed in the outer shell. The aerosol stream was neutralized in the inner shell and continued on to be contacted with the charged droplets in the deposition chamber. This dry, neutralized aerosol stream was monitored by a portable Matheson, Model 604, rotameter.

A third supply of laboratory air entered the deposition chamber as flush air and was monitored by a portable Matheson, Model 604, rotameter. Both the dry aerosol stream and the flushing air stream left the deposition chamber at the flushing air exit and continued to the drain.

The third section of the experimental apparatus is the deposition chamber itself (see Figure 4). This plexiglass cubicle was 4 inches x 4 inches x 4-7/16 inches tall and was composed of three compartments. The top compartment housed the absorption chamber. This compartment was filled with the dry aerosol and was the place where the charged droplets contacted the aerosol. The middle compartment

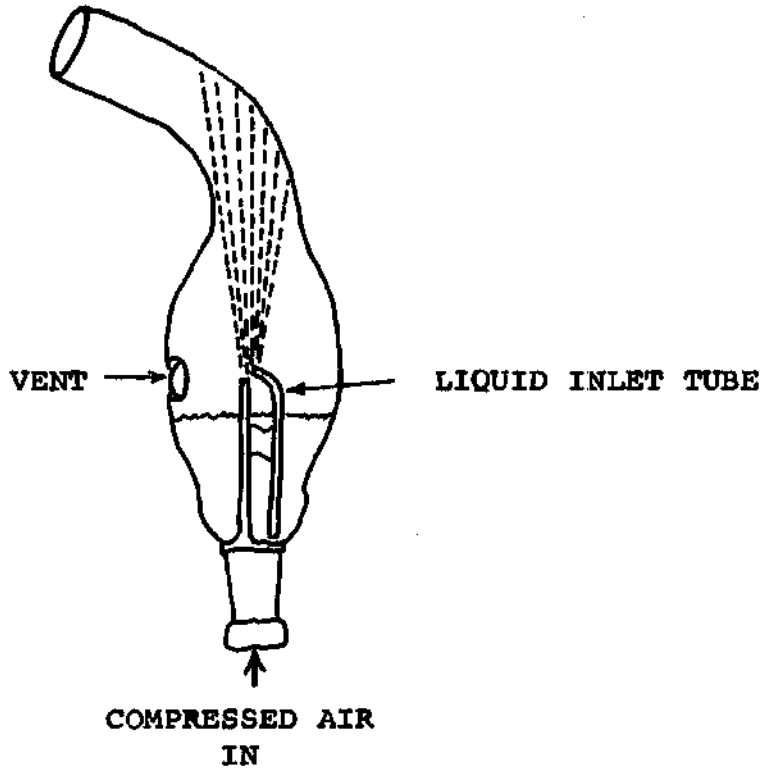

Figure 3. Diagram of the Aerosol Generator

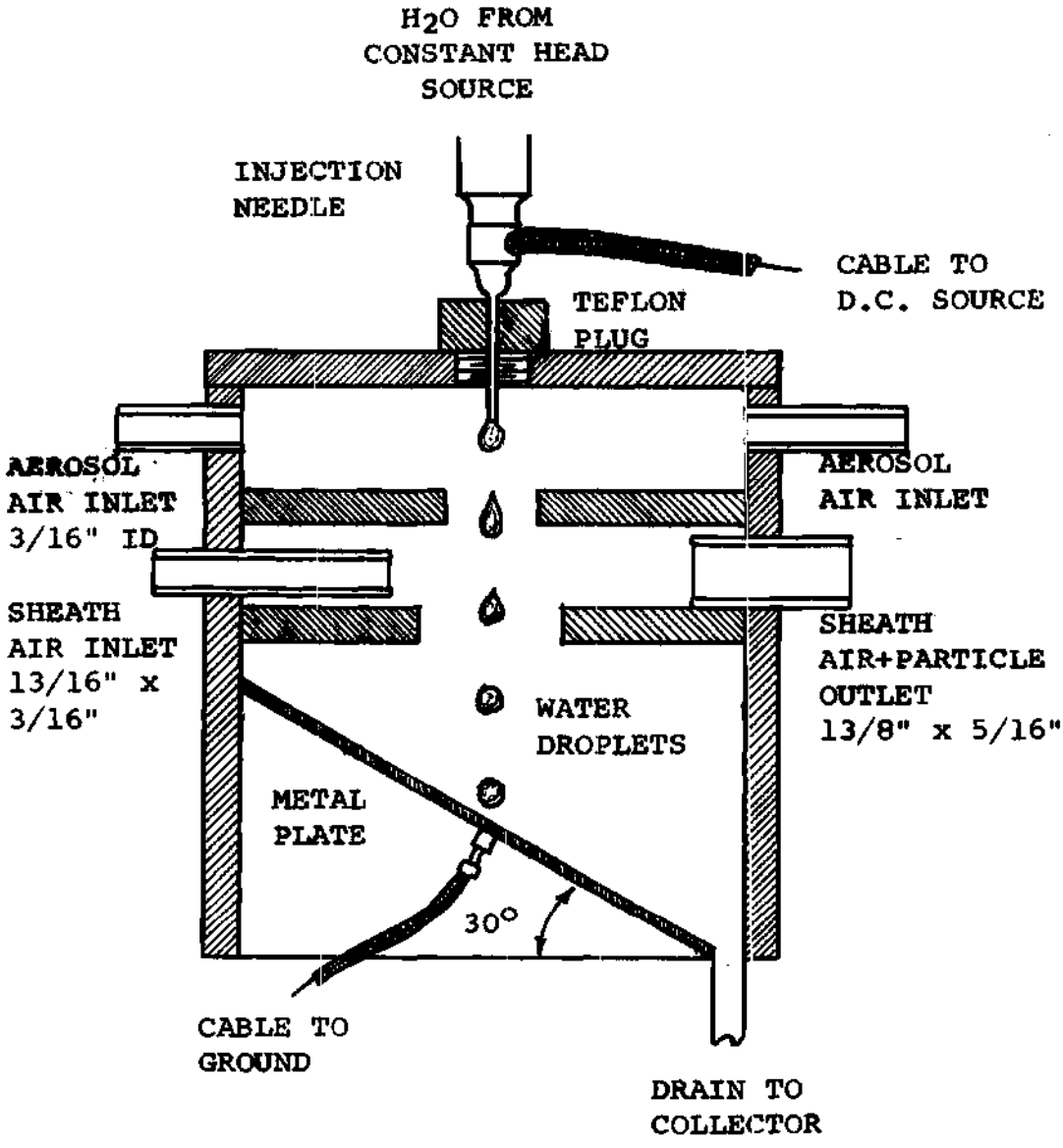

Figure 4. Diagram of the Deposition Chamber

housed the flushing chamber. Flushing air entered this compartment from its inlet side through a nozzle and exited through a large outlet nozzle directly across the chamber from the inlet nozzle. The flushing air then left the deposition chamber and swept the dry aerosol stream along with it to the drain. The lower compartment housed the collection chamber. In this compartment, the exposed charged droplets were collected.

At the base of the collection chamber was a stainless steel plate fitted with a short stainless steel drain tube and electrically connected to the outside. A sealant made secure all metal-to-plexiglass joints. The hypodermic needle was inserted into a Teflon plug which screwed into the top of the deposition chamber and served as an electrical insulator. Concentric holes in the compartment divider allowed the droplets from the needle to fall onto the stainless steel base plate of the collection chamber and then out the drain tube to a collection flask. Any contact of the aerosol with the water resting on the stainless steel plate was prevented by the flushing air.

The fourth section of the experimental apparatus consisted of the equipment and instrumentation to measure the droplet parameters. This section included a Condensor Product glass capacitor; Keithley, Model 610A, electrometer; Keithley, Model 6103A, voltage divider; Honeywell digital voltmeter; a standard timer; and a Matheson, Model 601,

rotameter. The drop rate was obtained by measuring the time required for 10 drops to fall with the timer.

To measure the charge delivered by the droplets, the stainless steel plate was wired to the capacitor and the capacitor stored the charge. The capacitor voltage was monitored by the electrometer which was plugged into the digital voltmeter. The RC time constant for the capacitive circuit was found to be 3410 ± 25 seconds. A 1000:1 ratio voltage divider attached to the electrometer measured the voltage to the needle which never exceeded 4 kv.

The final section of the experimental apparatus consisted of the equipment used to collect and analyze the exposed charged droplets. This section consisted of several 250 ml and 125 ml flasks, two Beckman pyrex rectangular cells, and a Beckman, Model B, spectrophotometer. When sufficient water had collected in the collection flask below the collection chamber, the collection flask was removed and its contents were poured into a Beckman pyrex rectangular cell for analysis in the spectrophotometer. This instrument measures the amount of light transmittance of a sample and is discussed further in Appendix 1. The amount of transmittance is directly proportional to the amount of particles present in the sample. From this measurement, the concentration of the latex particles in the sample was determined.

The previous explanations of the experimental apparatus do not fully specify the function of each piece of equipment;

however, these functions will become clearer in subsequent chapters.

CHAPTER III

PROCEDURE AND DATA ANALYSIS

Prior to making an experimental test several instruments required warm-up time. The electrometer, digital voltmeter, and spectrophotometer were all turned on at least thirty minutes prior to their use. After this time, the Matheson, Model 604, rotameter was used to set the aerosol stream at 115 mm (stainless steel ball) and the flush air stream at 100 mm (glass ball). The water flow rate was set around 80 mm (glass ball) with a Matheson, Model 601, rotameter. The high voltage source was then turned on and the voltage applied to the needle was measured with the high voltage divider and the electrometer. Next the spectrophotometer reading was set to 100% transmittance for a pure distilled water sample (blank). Finally, all water from the collection chamber was drained to a polyethylene jug on the floor.

When the test had been in progress about ten minutes, a collection flask was attached to the drain line from the collection chamber. The flow rates of all streams and the temperature of the droplet reservoir were recorded. A measurement of the drop rate was then made by measuring the time required for 10 drops to fall with the timer. Next, the voltage gain across the capacitor was measured by the

electrometer with values being recorded every ten seconds for forty seconds. After checking the flow rates again for constancy, approximately ten minutes were allowed for sufficient water to collect in the collection flask. After ten minutes, the collection flask was removed and the collection chamber drain line was inserted into the polyethylene jug.

The collected water was then ready for analysis. The spectrophotometer was once again checked for 100% transmittance with the distilled water sample and adjusted as necessary. A portion of the collected water was then poured into a Beckman pyrex rectangular cell and placed inside the spectrophotometer for analysis. A reading was taken, recorded, and checked. From this reading the concentration of latex particles in the collected water was determined by noting the concentration corresponding to the particular transmittance on the spectrophotometer calibration curves (see Figures 23 to 36).

While the sample was being analyzed, the streams were left running to obtain stability for the next test. This would start after the applied voltage was changed and the collection flask inserted at the end of the collection chamber drain line. This completes the description of a typical experimental test.

Experimental tests were made on seven different latex particle diameters. These diameters expressed in micrometers

are as follows: 0.176, 0.312, 0.481, 0.822, 1.101, 2.020, and 5.700. Each particle diameter was exposed to water droplets with positive and negative voltages at the following settings: 0.5 kv, 1.50 kv, 2.50 kv, 3.00 kv, and 4.0 kv. In addition, prior to each set of positive and negative voltage tests, a test was made at zero voltage. To check for reproducibility, each particle diameter had two sets of positive voltages and two sets of negative voltages.

After the above tests were completed, the collected data were analyzed. The only errors present in the system were reading errors and systematic errors. The latter type is due to instruments out of calibration. This type of error was prevented by checking the instruments against reliable standards. The electrometer was found to be accurate when it was calibrated against a fixed voltage standard furnished by Honeywell for calibration of the digital voltmeter. A measured volume of gas which passed at a constant rate by water displacement was used to calibrate the air flow rotameters.

The factory curves which accompanied the rotameters were accurate. By observing the amount of water delivered in a given time, the rotameter which measured the flow-rate through the needle was calibrated. A wheatstone bridge circuit was used to measure the glass capacitor and determined its capacitance to be 4.88×10^{-9} farads at 1000 Hz. Finally, the RC time constant was determined to be

3410 ± 25 seconds. This implied a good isolation electrical resistance at 6.98×10^{11} ohms.

Concerning the validity of the data obtained in these experiments, two important assumptions were made. The first assumption was that no aerosol was collected by the residual water on the steel plate of the collection chamber. To verify this assumption, samples that had been previously analyzed were rechecked by placing them in the collection chamber again and allowing them to remain there for the typical time of a test, viz., ten minutes. Except for the water supply being shut off, the test was carried out in the usual manner. The water was then removed and analyzed again. There was very little measurable difference in the samples and the values obtained fell within the scatter present in the data. The second assumption was that the charge on the water droplets when no voltage was applied was zero. To verify this assumption, several tests were made at zero voltage and the voltage gains across the capacitor were measured by the electrometer. These voltage gains were relatively small when compared with voltage gains obtained at the lowest voltage of 0.5 kv.

The procedure in which the collected data was used to obtain the parameters of interest in this study will now be presented. The nomenclature used for both the measured and calculated parameters are listed in Table 1. One most important parameter in the study was the surface charge

density, q, and the amount of aerosol deposited per unit area of droplet, C_a. Of secondary significance were the collection parameter, K_I, and the collection efficiency, E.

To obtain the surface charge density, the radius of the droplet was needed. It was obtained from the expression

$$R = \left(\frac{F_w}{80\pi x DR}\right)^{1/3} \tag{4}$$

where F_w is the volumetric flowrate of water and DR is the drop rate.

The surface charge density, q, was then calculated using

$$q = \frac{Q_o}{4\pi R^2 (DR)} \tag{5}$$

where Q_o is the charge delivery rate or current to the steel plate. The value Q_o was obtained from the capacitor charging curve

$$Q_o = \frac{(V_c)}{R_s} \left[1-\exp\left(-\frac{tc}{R_s c_e}\right)\right]^{-1} \tag{6}$$

where R_s is the system resistance, V_c is the voltage across the capacitor at the time t_c and c_e is the capacitance. V_c is equal to V/s, the slope of the capacitor charging curve, times one second when t_c is one second. Equation 6

is derived in Appendix 2.

The amount of aerosol collected per unit area of droplet, C_a, was obtained from the expression

$$C_a = \frac{F_w \times \rho \times \text{concentration (\% solids by volume)}}{DR \times 60 \times 4\pi R^2 \times 100\%} \qquad (7)$$

where F_w is the volumetric flowrate of water, ρ is the density of water, concentration (% solids by volume) is taken from the spectrophotometer calibration curves, DR is the drop rate, and R is the radius of the droplet.

In order to compare the various C_a's, the amount of aerosol collected per unit droplet, C_p, was obtained from the expression

$$C_p = \frac{F_w \times \text{concentration (particles/cc)}}{DR \times 60 \times 4\pi R^2} \qquad (8)$$

where F_w is the volumetric flow rate of water, concentration (particles/cc) is taken from the spectrophotometer calibration curves, DR is the drop rate, and R is the radius of the droplet.

The relative velocity, U_o, between the droplet and the aerosol was taken as just the velocity at which the water was dispensed from the needle's tip. Since the aerosol entered the chamber on four sides through inlets located opposite

one another, it was assumed that the velocity of the aerosol particles was small compared with the velocity of the water entering the chamber. U_o was then calculated by dividing the flow rate of water through the needle, F_w, by the cross-sectional area of the needle's tip, A.

The collection parameter, K_I, was obtained using Equation 2, repeated here

$$K_I = \frac{X_s - 1}{X_s + 2} \frac{4Cr^2q^2}{3\epsilon_o RNU_o}$$

The Cunningham factor, C, in Equation 2, was calculated from the expression

$$C = 1 + \left(\frac{2}{PxD_p}\right) [6.32 + 2.01 \exp(-0.1095\ PxD_p)] \qquad (9)$$

where P is the air pressure in cm of Hg and D_p is the diameter of the particle in micrometers [23].

The collector efficiency, E, was calculated in the following manner: the efficiency was defined as the ratio of the amount of aerosol particles collected when the droplet carried a surface charge, C_a, to the amount collected when there was no surface charge, C_o, that is $E = C_a/C_o$. When no surface charge was present, E was equal to one.

The final topic of discussion is the error produced in the calculated results by random error associated with

the reading of instrument scales. The surface charge density, q, was a function of V_c, R_s, t_c, DR, F_w, and C_e. In this case, the standard deviation in q is equal to the square root of the sum of the squares of the standard deviations of the parameters involved [24]. These deviations are the same ones used by Lewis [20] and are

$$d(C_e) = 0.2\% \qquad d(V_c) = 1\%$$
$$d(R_s) = 0.8\% \qquad d(t_c) = 1\%$$
$$d(DR) = 0.3\% \qquad d(F_w) = 1.5\%$$
$$\therefore d(q) = 2.5\%$$

The amount of aerosol collected, C_a, was a function of SR, F_w, and DR. Since the variation in F_w and DR will cancel for the most part, the contribution of each of these will be reduced by one half. The calibration curve was a best straight line fit, so the error involved in this calculation should also be included. These deviations are the same ones used by Lewis [20] and are

$$1/2\ d(F_w) = 0.75\% \qquad d(SR) = 0.5\%$$
$$1/2\ d(DR) = 0.15\% \qquad d(Bsl) = 0.1\%$$
$$\therefore d(C_a) = 0.9\%$$

The collection parameter, K_I, was a function of q, r, F_w, and DR. The approximate deviations are

$$d(q) = 2.5\% \qquad d(r) = 2.33\%$$

$$d(F_w) = 1.5\% \qquad d(DR) = 0.3\%$$

$$\therefore d(K_I) = 6.29\%$$

The above deviations are the same ones used by Lewis [20].

CHAPTER IV

DISCUSSION OF RESULTS

The experimentally measured parameters for all tests are listed in Appendix 3. The calculated parameters for all tests are listed in Appendix 4.

Before describing the individual graphs, some comments will be made about the data. First of all, with any aerosol cloud experimentation is difficult. Large distances between the aerosol generator and the reaction chamber allow time for particle coagulation, loss of particles to the walls of the dryer, the neutralizer, and tubing, and clogging of the lines. These conditions can usually produce fluctuations in the aerosol flow rate; however, fluctuations in the aerosol flow rate were not noticeable in this study. In addition, the water flow rate varied slightly from test to test. This variation, however, was not of sufficient significance to require special accounting.

Secondly, any foreign material gives a spectrophotometer reading. Although distilled water was used exclusively in the experiments, it was not known if any corrosion products had entered the water stream from the stainless steel hypodermic needle, stopcock, and metallic plate. Since the needle, stopcock and metallic plate were cleaned prior to

every test, errors due to corrosion products were considered small.

Thirdly, some consideration was given to the slight build up of particles on the exposed needle. When a lesser voltage was applied following a test in which a higher voltage had been applied, it was not known if some of the particles which had been deposited on the needle were knocked off through collisions with other aerosol particles in the stream and then deposited on the droplets being formed or those in the collection chamber. Since the electrostatic attraction was no longer as strong as in the preceding test, this occurrence was thought to be of little significance because the flushing air stream was assumed to be effective in sweeping out the unused aerosol particles. This assumption was not completely valid because some aerosol was deposited on the water in the collection chamber. This fact was tested by placing plain distilled water in the collection chamber, letting it remain there for the time of a typical test, and analyzing it afterwards. The amount deposited in the collection chamber was similar to the amount obtained for zero charge on the droplets.

Another point of interest is the Kr-85 aerosol charge neutralizer. This 2 millicurie source was used to neutralize the aerosol particles prior to their entrance to the collection chamber; however, no measurements were made of the charge on these particles before or after the neutralizer.

It can only be assumed, based on the work of Liu and Pui [22], that sufficient time was allowed for neutralization of the aerosol particles in the neutralizer. The drift of the spectrophotometer needle was an area of concern. The needle which indicated per cent transmittance initially fluctuated between one to three percent. Some of this fluctuation was eliminated by checking vital electrical contacts in the spectrophotometer and grounding it; however, after all this, approximately a one percent fluctuation remained.

In the initial set-up of the equipment, the collecting flask between the aerosol generator and the dryer tended to knock out too many aerosol particles by impaction. This flask was then removed and the aerosol generator was attached directly to the dryer.

Still another point is the fact that the amount of solution in the aerosol generator changed with time. As time passed the solution became more concentrated; therefore, the mass distribution of the aerosol probably changed with time. This change was lessened to a certain extent by placing a new solution in the generator after it reached a certain volume. No correction in the data was made for this phenomena.

Finally, any kind of foreign material either in the water to be analyzed or on the rectangular cells, even finger prints, could alter the results obtained significantly. This effect was ignored since every practical precaution against

the accidental insertion of foreign materials in the sample or in the rectangular cells was taken.

All of the previous points were mentioned to aid in understanding the scatter in the data. With these points in mind, the explanation of the various curves can commence.

The data representing the effect of surface charge on the deposition of aerosol is presented in Figures 5, 6, 7, 8, 9, 10, 11, 12, and 13. Each figure is entitled C_a or C_p *vs.* q^2. These figures show the relationship of C_a or C_p to q^2 for different aerosol particle sizes. As these graphs show, there is no exact, constant relationship between the collected aerosol and the surface charge on the droplets.

In Figure 5, the positively charged droplets have higher collected aerosols and increase the collected aerosol with increasing surface charge density. The negatively charged droplets have approximately the same collected aerosol with increasing surface charge density. The positively charged droplets in Figure 6 at first increase their collected aerosol with increasing surface charge density and then decrease. This same pattern is typical of the negatively charged droplets; however, these droplets reach higher collected aerosol values.

In Figure 7, the positively charged droplets maintain approximately the same surface charge density but fluctuate in collected aerosol. The negatively charged droplets have the same pattern as in Figure 6, i.e., parabolic. Both the

positively and negatively charge droplets in Figure 8 have their collected aerosol decreasing with increasing surface charge density. The parabolic profile is evident once again for the positively charged droplets in Figure 9. The negatively charged droplets in this figure have their collected aerosol increasing with increasing surface charge density.

In Figure 10, the positively charged droplets have their collected aerosol first increasing with surface charge and then decreasing. The negatively charged droplets follow just the opposite pattern of the positively charged droplets. The positively charged droplets in Figure 11 tended to stay in the same collected aerosol range with increasing surface charge density. On the other hand, the negatively charged droplets decreased their collected aerosol with increasing surface charge density.

In order to compare the various C_a's, all of the positively and negatively charged droplet points are plotted as C_p *vs.* q^2 in Figures 12 and 13, respectively. Most of these points showed an increase in collected aerosol with increasing surface charge; however, after a certain amount of surface charge density, no further changes in collected aerosol were noted. Greater aerosol collection was obtained when the particle diameters were 0.176 micrometers and 0.312 micrometers.

Some explanation for the scatter in the C_a and C_p *vs.*

q^2 graphs may be found in the previous work. For example, Walton and Woolcock [9], observed that the collection of dust particles of less than 2.5 micrometers diameter was extremely difficult to measure experimentally. In this particular study, no charge effect was present. On the other hand, Gunn and Hitschfeld's study [17] showed that the collection of particles with a diameter of about 15 micrometers had only 15% efficiency and implied that the efficiency decreased with the particle diameter.

It is interesting to note that the results obtained from the graphs of C_a and C_p *vs.* q^2 are similar to the results obtained by Lewis [20]. Lewis's graphs of C_a *vs.* q^2 showed a significant increase in the amount of deposited aerosol with increasing surface charge on the droplets and a slight increase in the amount of aerosol deposited when positive voltage was applied compared to when negative voltage was applied.

The next area of interest is the relationship between the collection parameter, K_I, and the collection efficiency, E. Both E and K_I are listed in Table 3. Figures 14, 15, 16, 17, 18, 19, and 20 show graphical representations of these values for each particle size. Figure 21 shows a graphical representation of E and K_I for all particle sizes.

The experimental data was least square fitted to straight lines. These lines had different slopes and intercepts for each particle size. Figures 14, 15, 18, 19, and 20

had lines with a positive slope and Figures 16 and 17 had lines with a negative slope. The intercepts for E at $K_I = 0$ ranged from .69 to 1.51.

In Figure 21, all of the experimental data was least square fitted to a straight line. This line has a slope of -.08 and an intercept of 1.08; therefore, in this study, the following expression represents the relationship between the collection efficiency, E, and the collection parameter, K_I:

$$E = 1.08 - .08 \times K_I \qquad (10)$$

The intercept in Equation 10 is very close to the theoretical intercept of one when no surface charge is present ($K_I = 0$). Unfortunately, the negative slope indicates that an increase in the surface charge on the water droplet will decrease the collection efficiency.

There are several possible reasons for the differences in the theoretical and experimental values. First of all, the aerosol used in this study was assumed to be neutral; however, the aerosol may be neutral with respect to the total aerosol cloud but it has a Boltzman Distribution of charged particles. These charged particles near a charged collector are influenced by both K_I and K_E; therefore, the actual collection parameter should be represented by $K = K_I - K_E$ because some of the particles were being repelled while others were being attracted. In addition, Kraemer and Johnstone [18]

observed greater deviation from their theory for the data obtained investigating K_I rather than using the corrected parameter, K. They also noted that for low collection efficiencies and small values of the parameters, the theory overestimates the collection efficiency.

In conclusion, the results obtained in this study show that in most cases there was an increase in collection efficiency with surface charge density; however, after a certain amount of surface charge density, no further changes in collection efficiency were noted. The results also demonstrate that the collection parameter of Kraemer and Johnstone [18], K_I, may be used to estimate the collection efficiencies of neutral aerosol particles on charged liquid spheres.

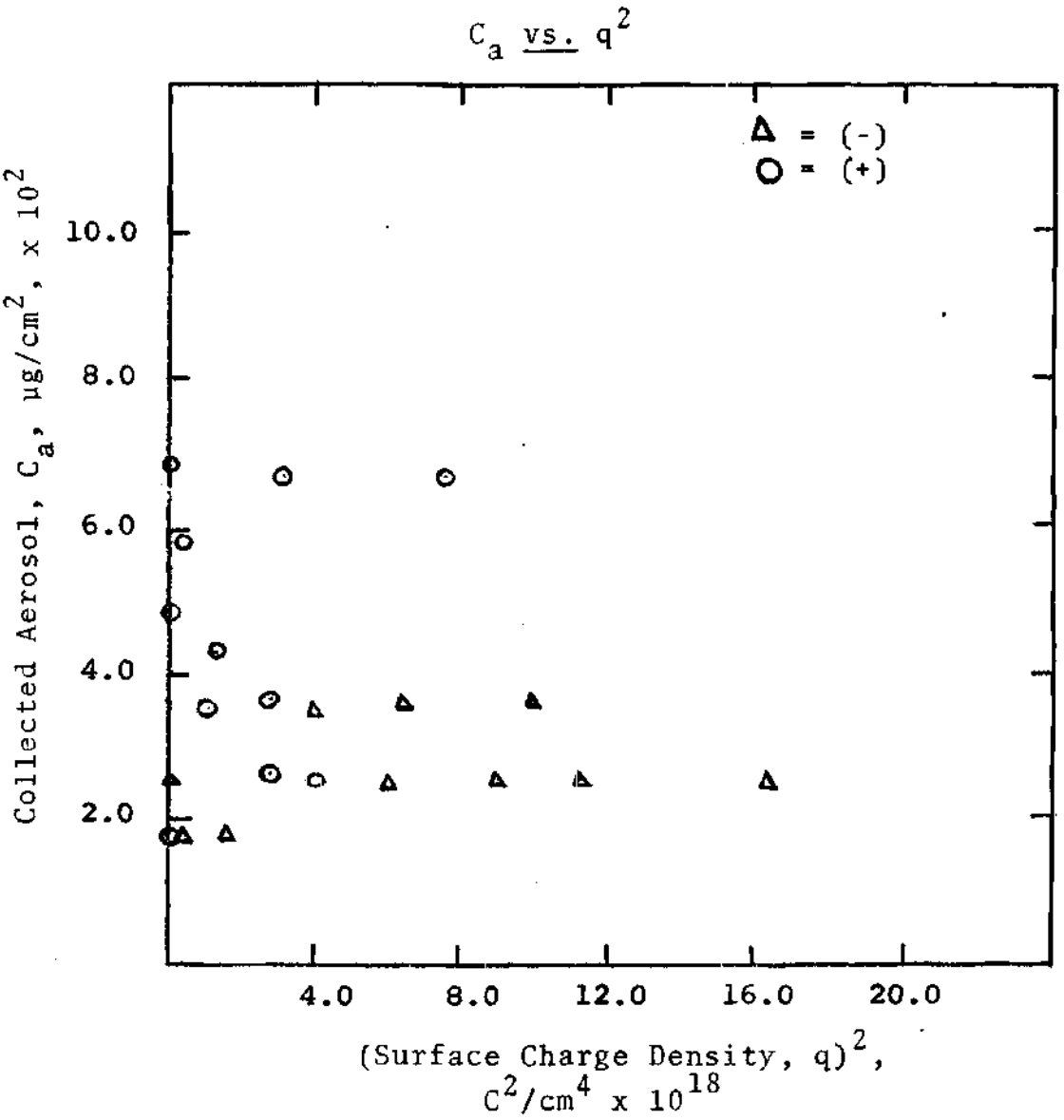

Figure 5. Graph of C_a vs. q^2 for Dp 0.176

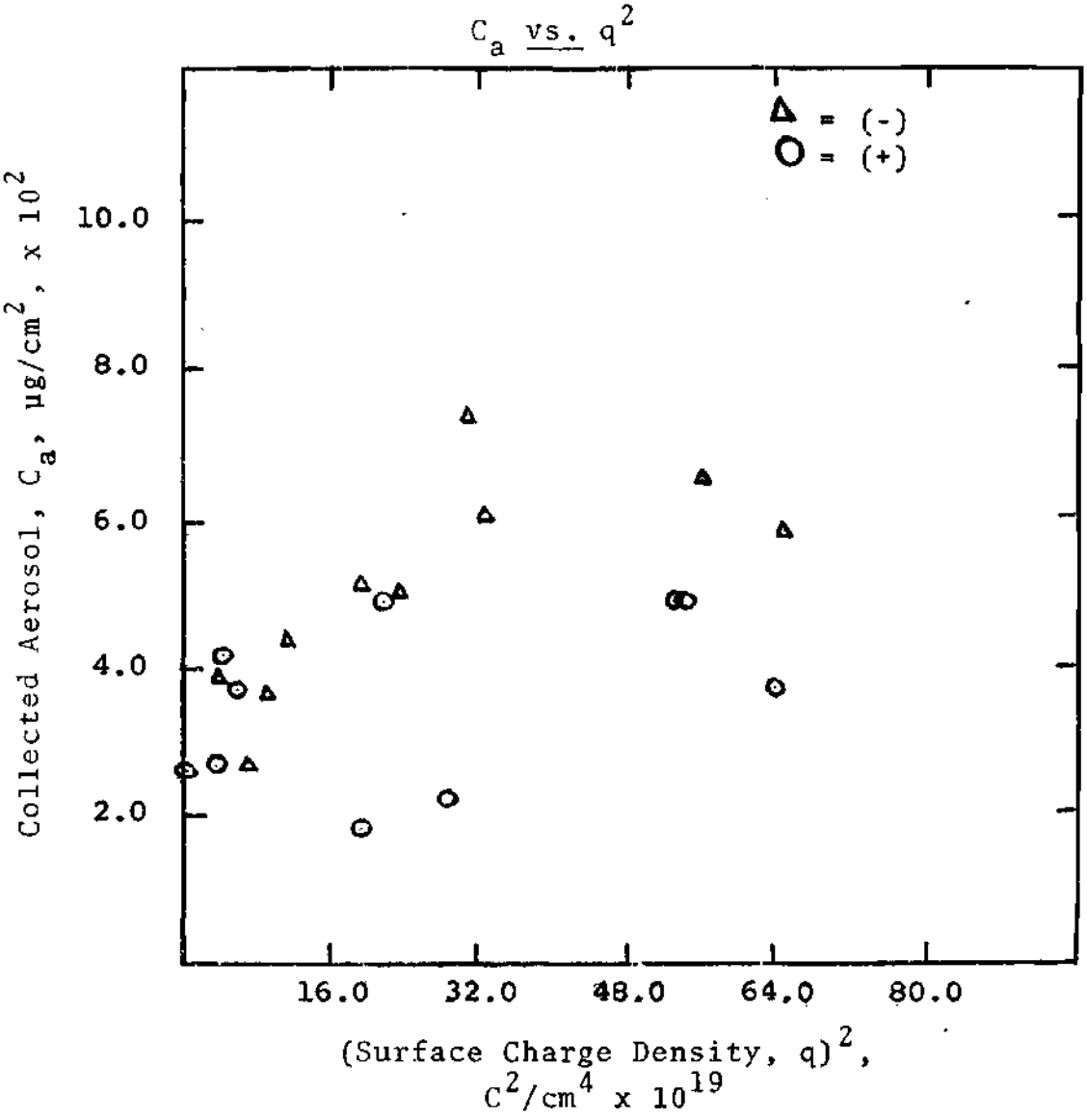

Figure 6. Graph of C_a vs. q^2 for D_p 0.312

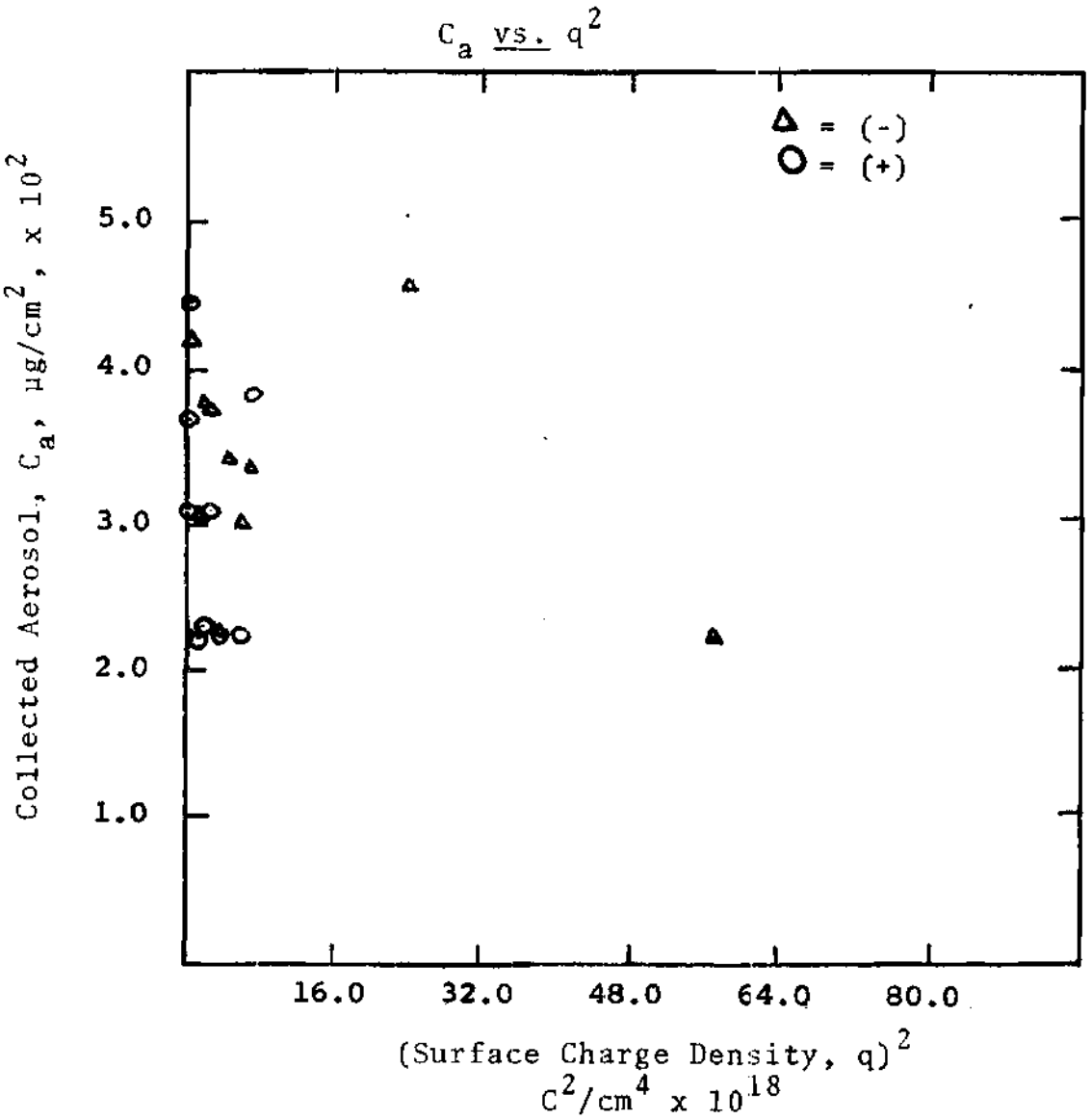

Figure 7. Graph of C_a vs. q^2 for D_p 0.481

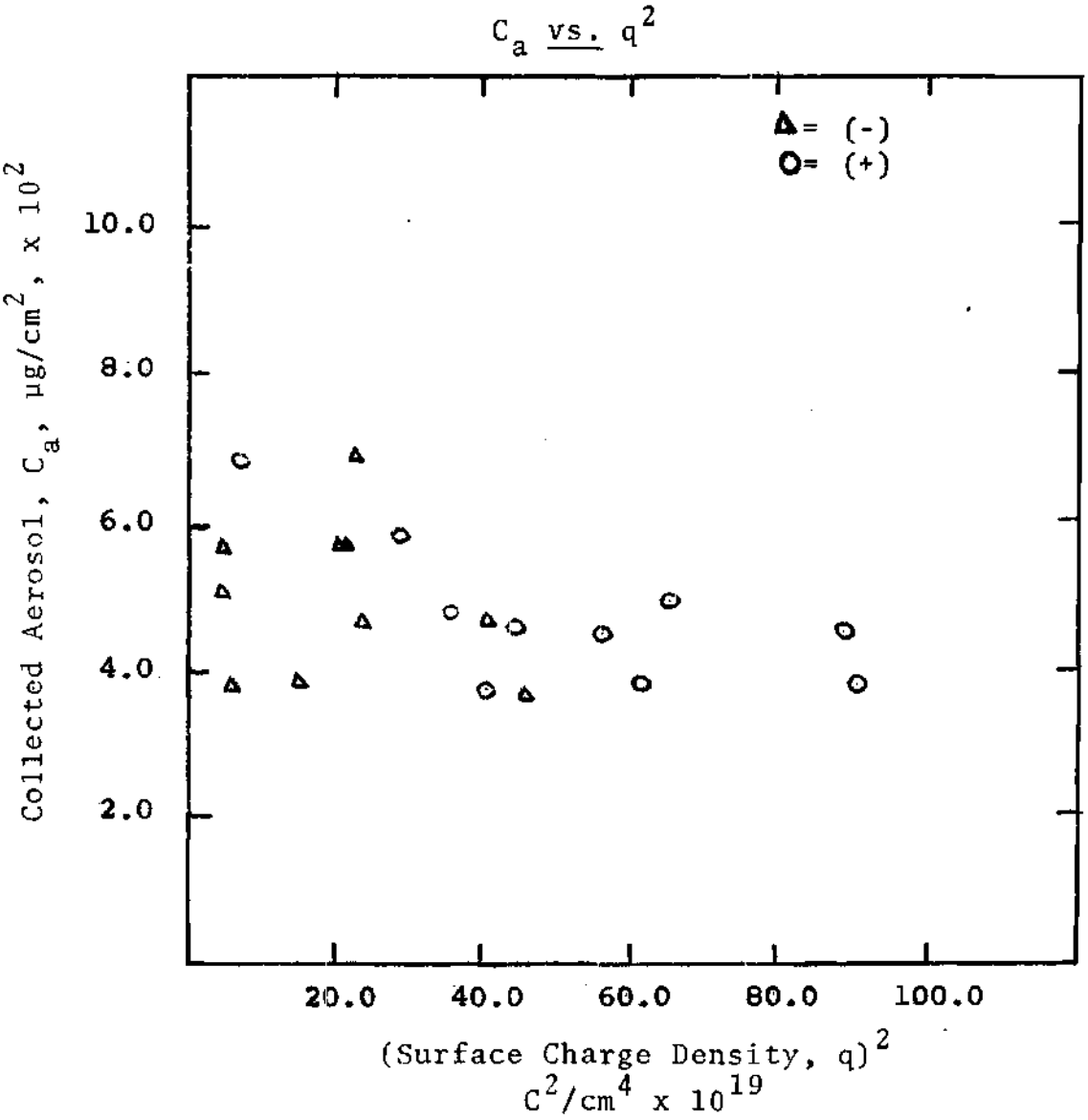

Figure 8. Graph of C_a vs. q^2 for D_p 0.822

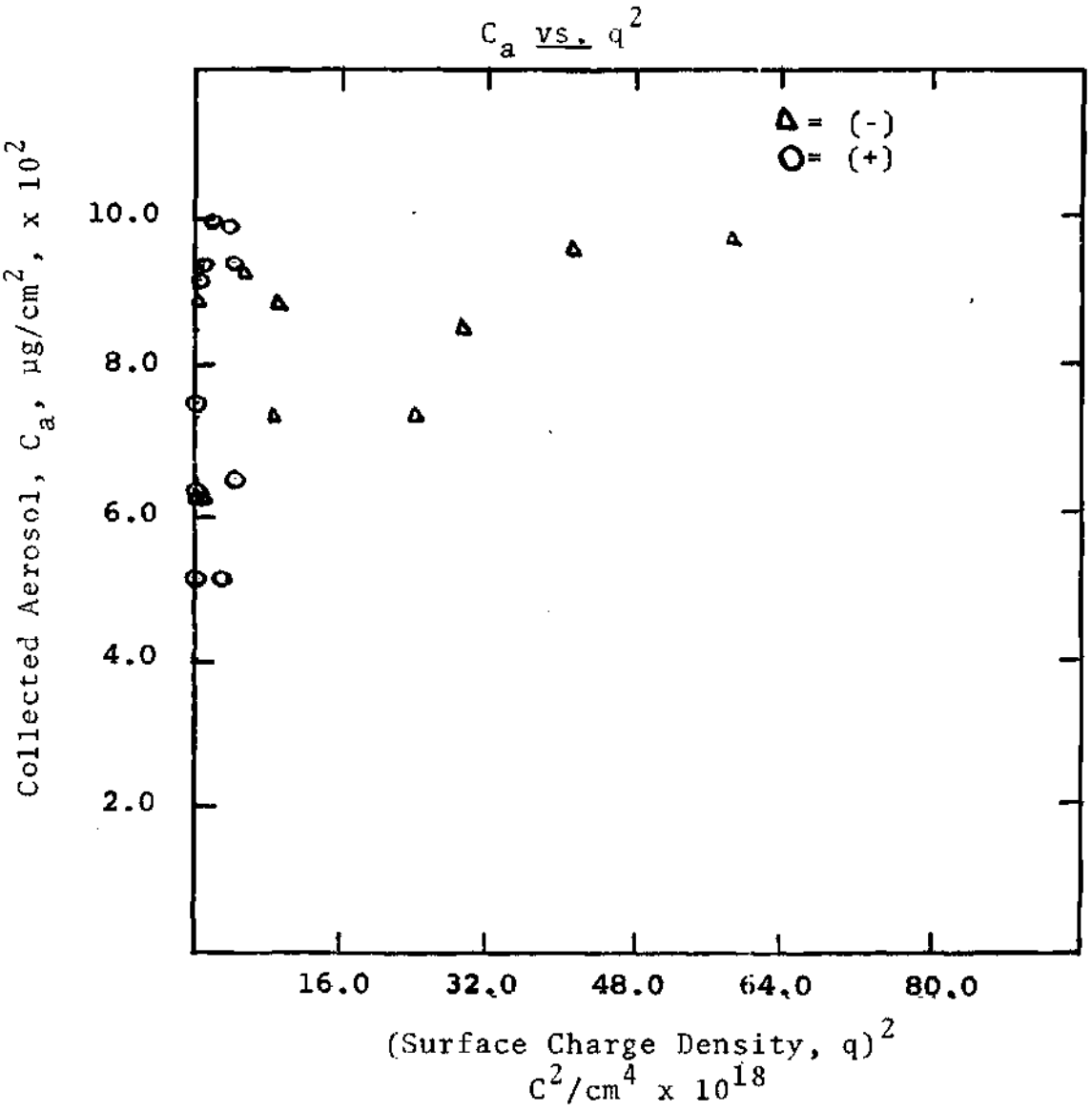

Figure 9. Graph of C_a vs. q^2 for D_p 1.101

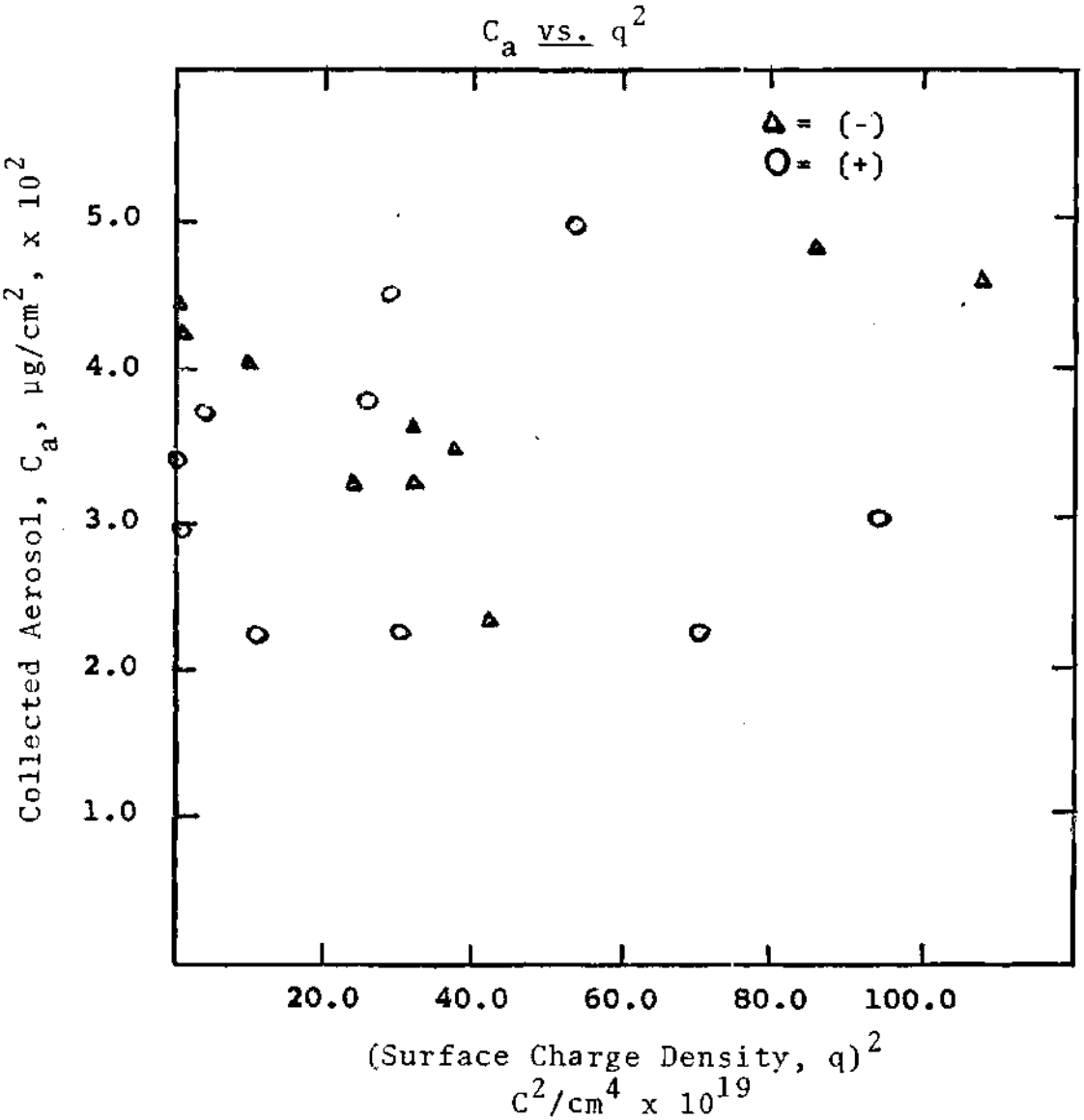

Figure 10. Graph of C_a vs. q^2 for D_p 2.020

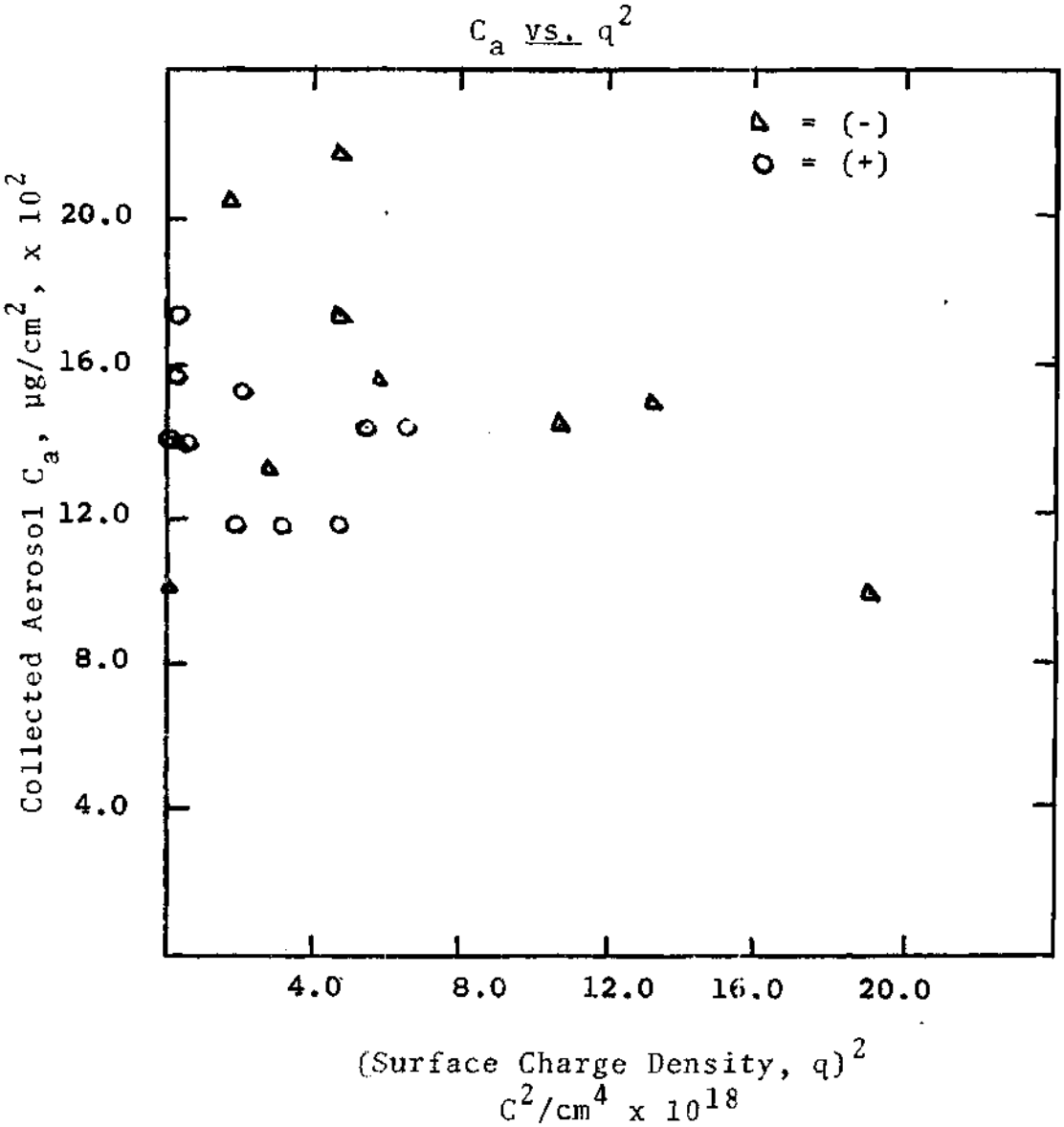

Figure 11. Graph of C_a vs. q^2 for D_p 5.700

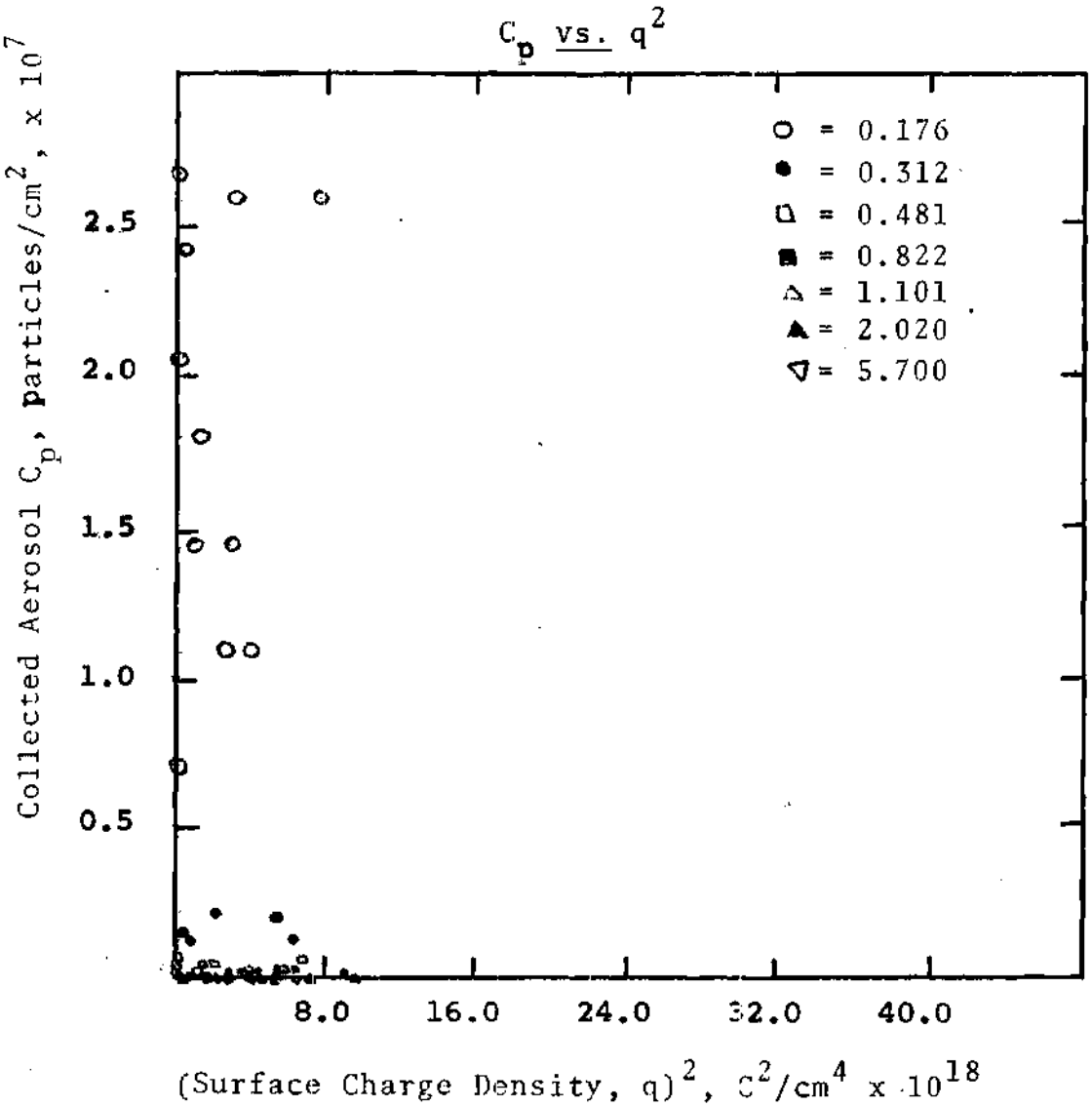

Figure 12. Graph of C_p vs. q^2 for + Charge

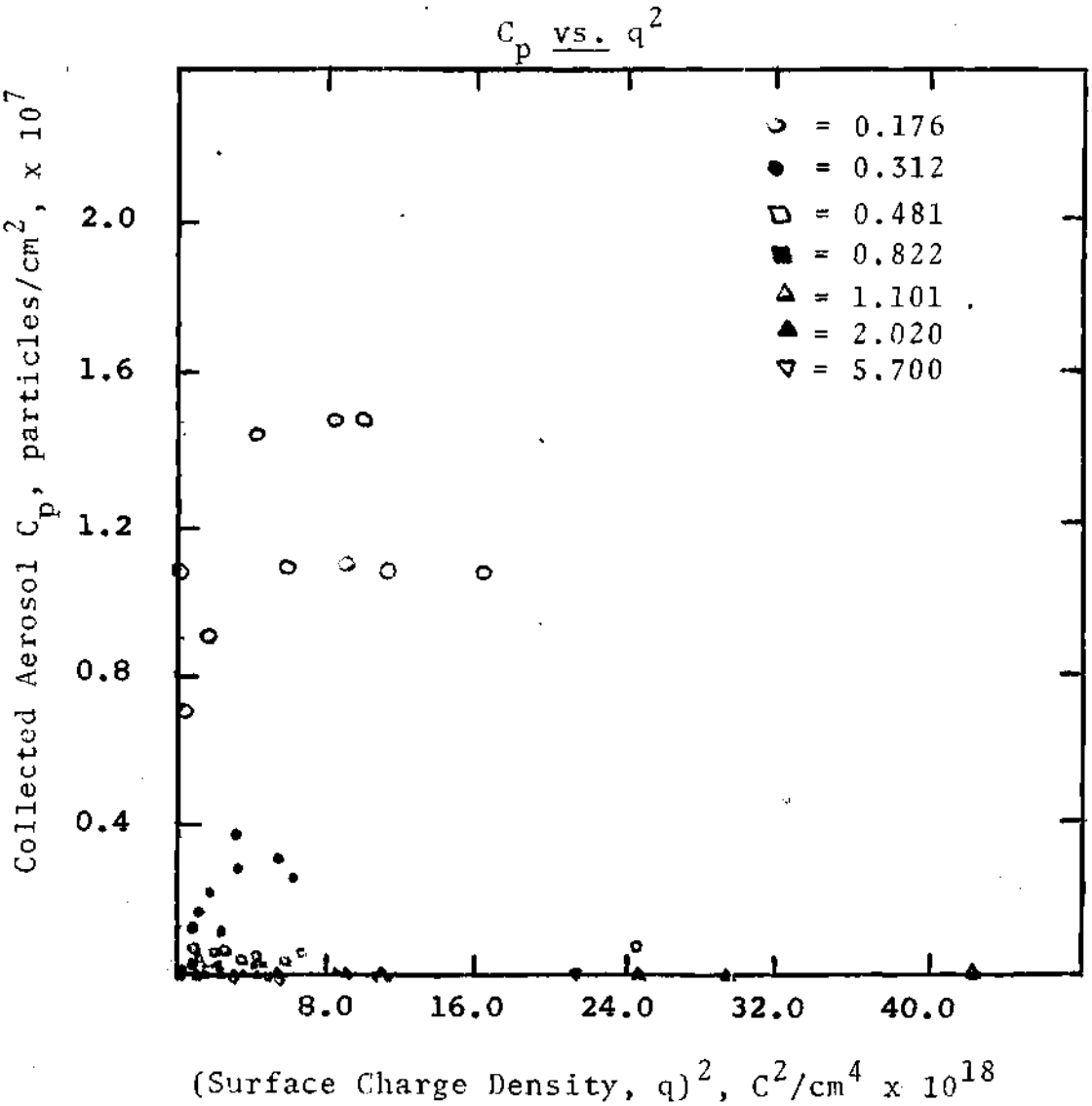

Figure 13. Graph of C_p vs. q^2 for - Charge

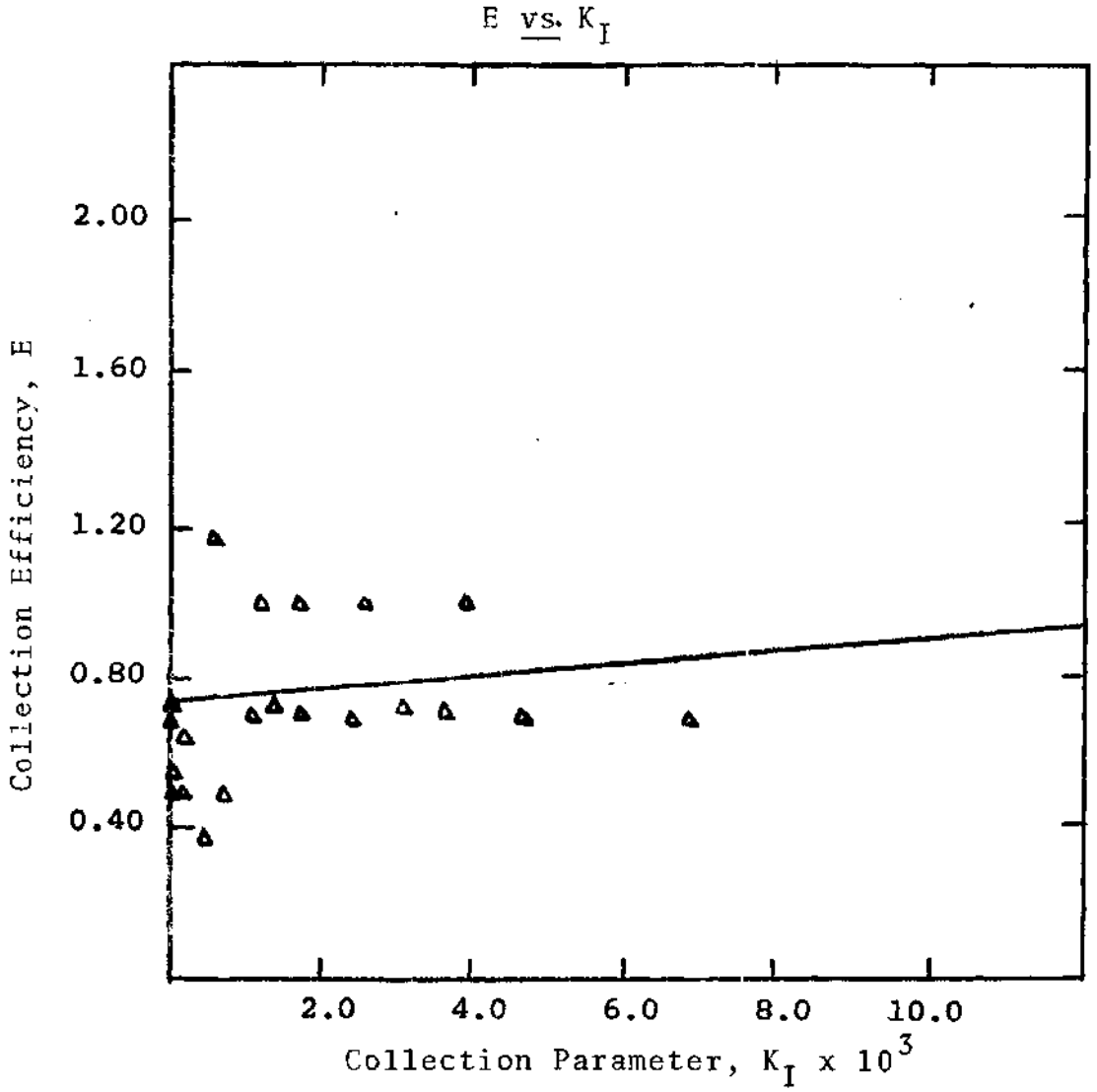

Figure 14. Graph of E vs. K_I for D_p 0.176

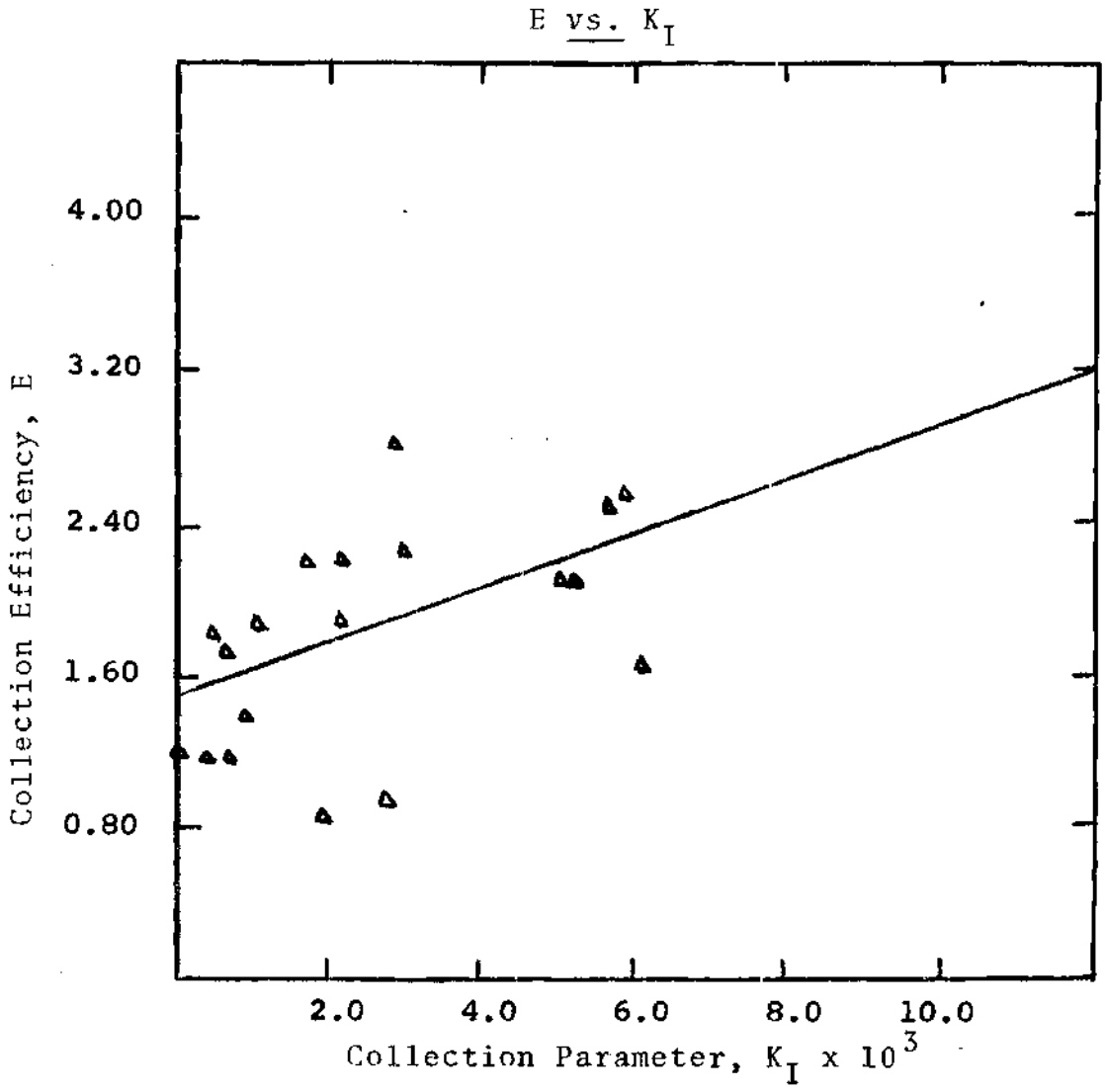

Figure 15. Graph of E vs. K_I for D_p 0.312

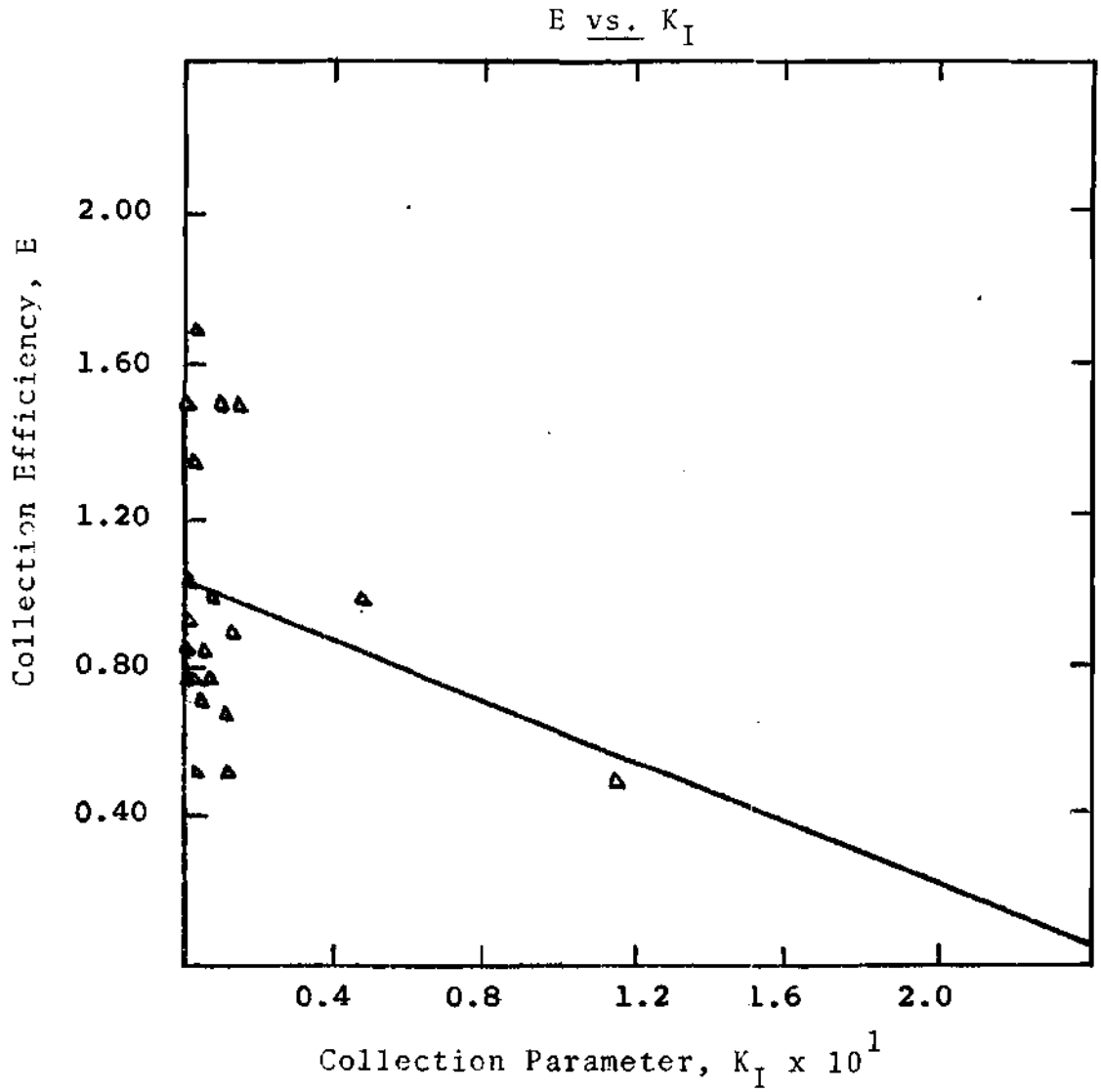

Figure 16. Graph of E vs. K_I for D_p 0.481

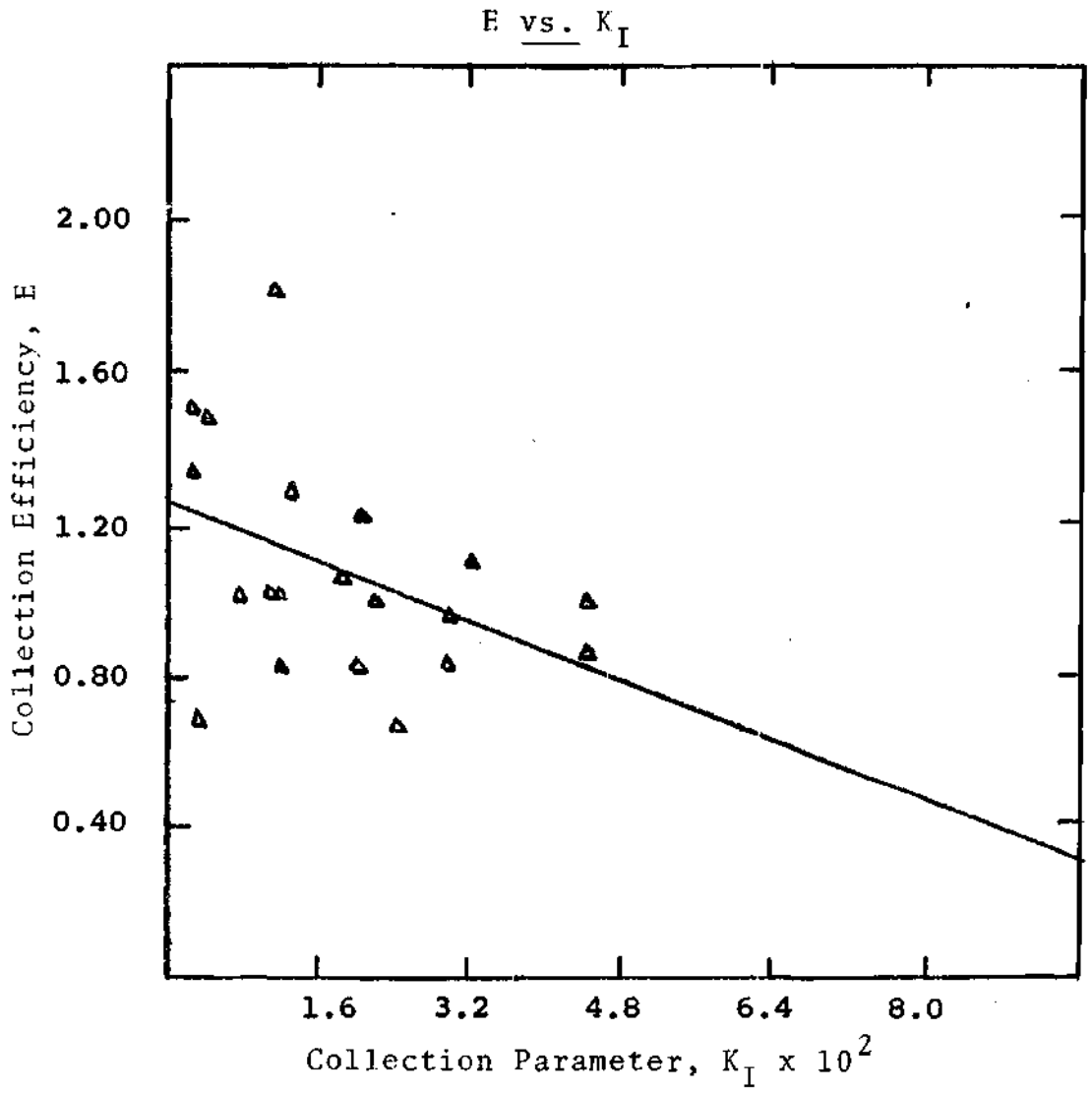

Figure 17. Graph of E vs. K_I for D_p 0.822

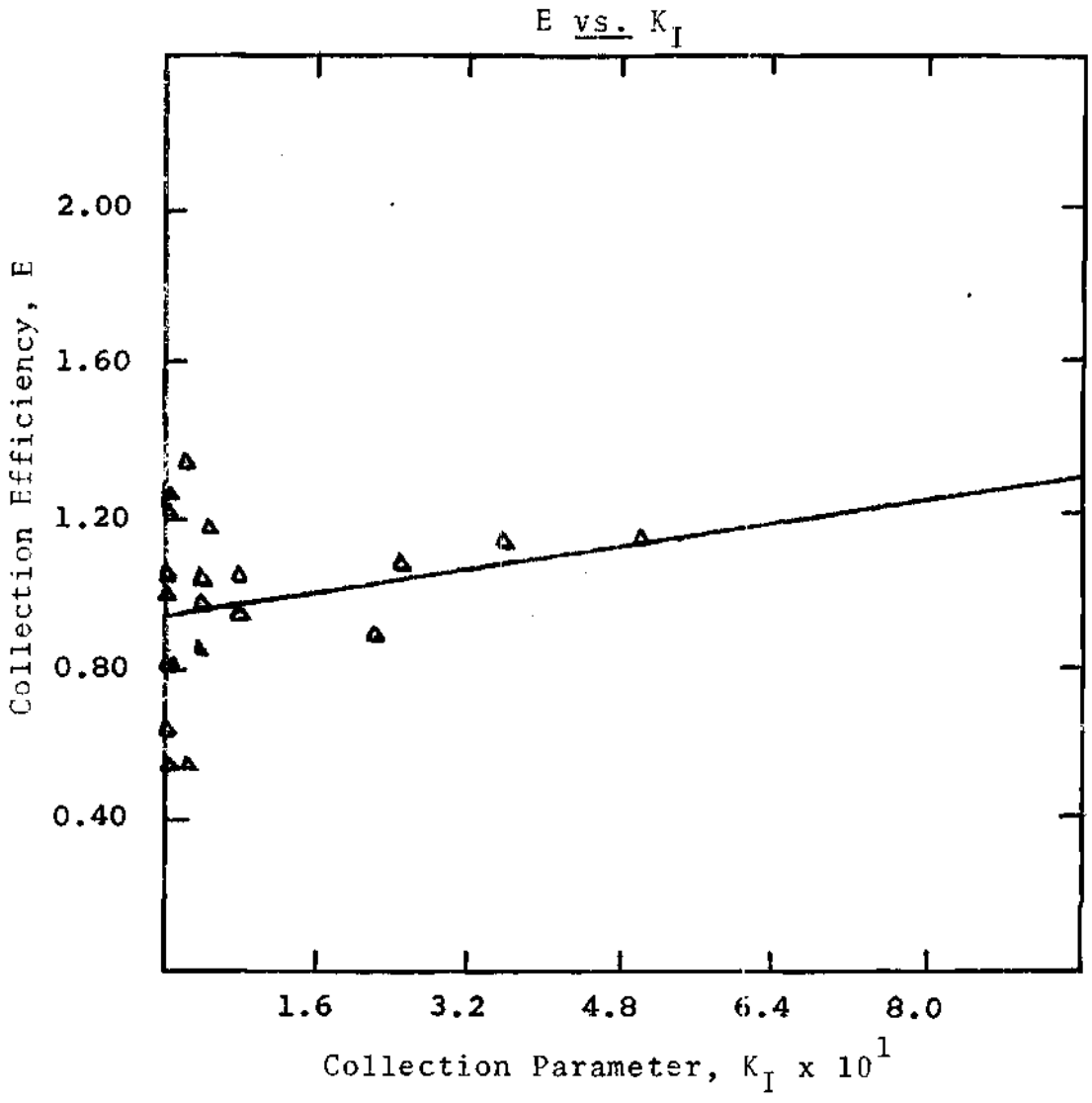

Figure 18. Graph of E vs. K_I for D_p 1.101

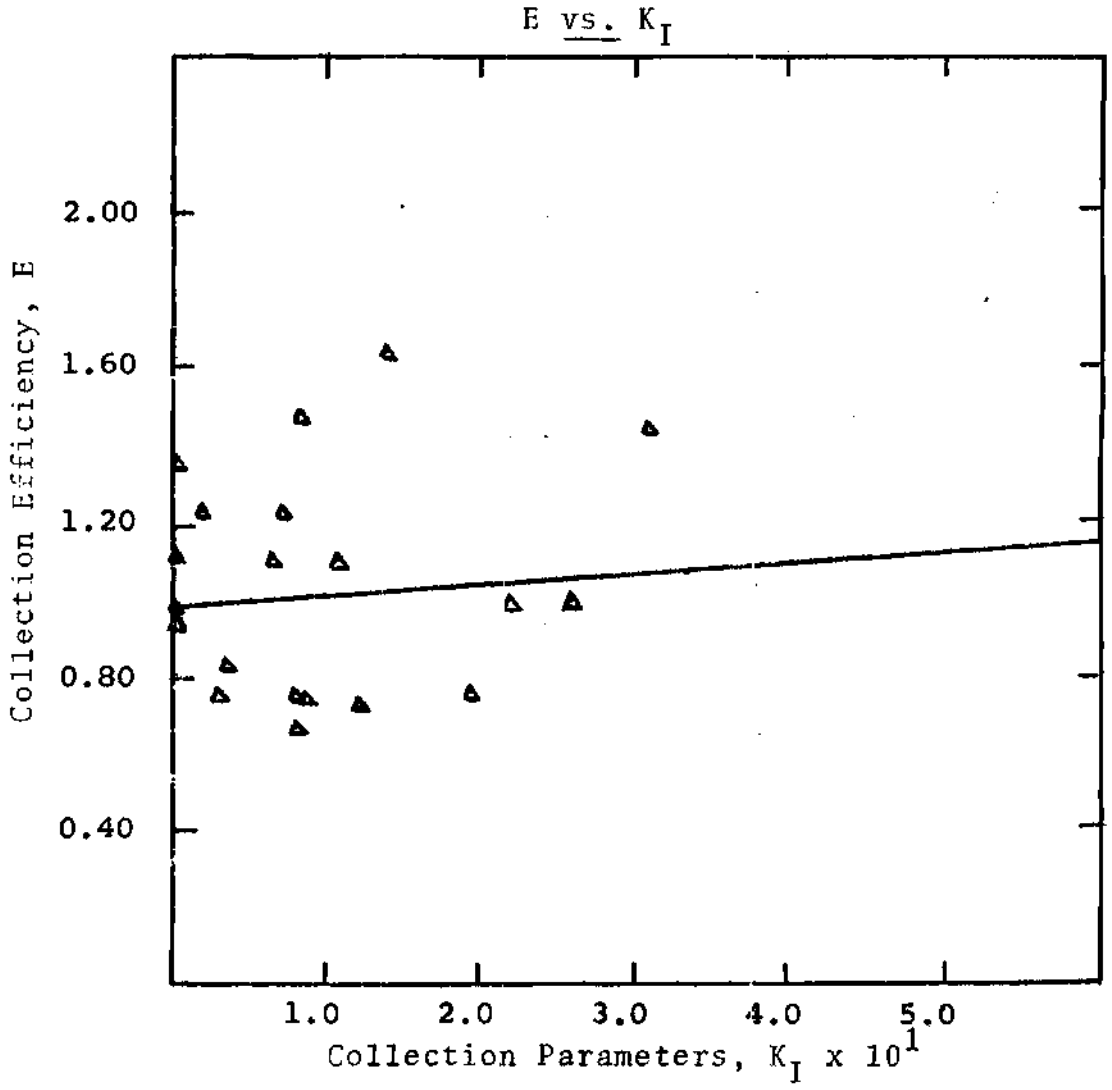

Figure 19. Graph of E vs. K_I for D_p 2.020

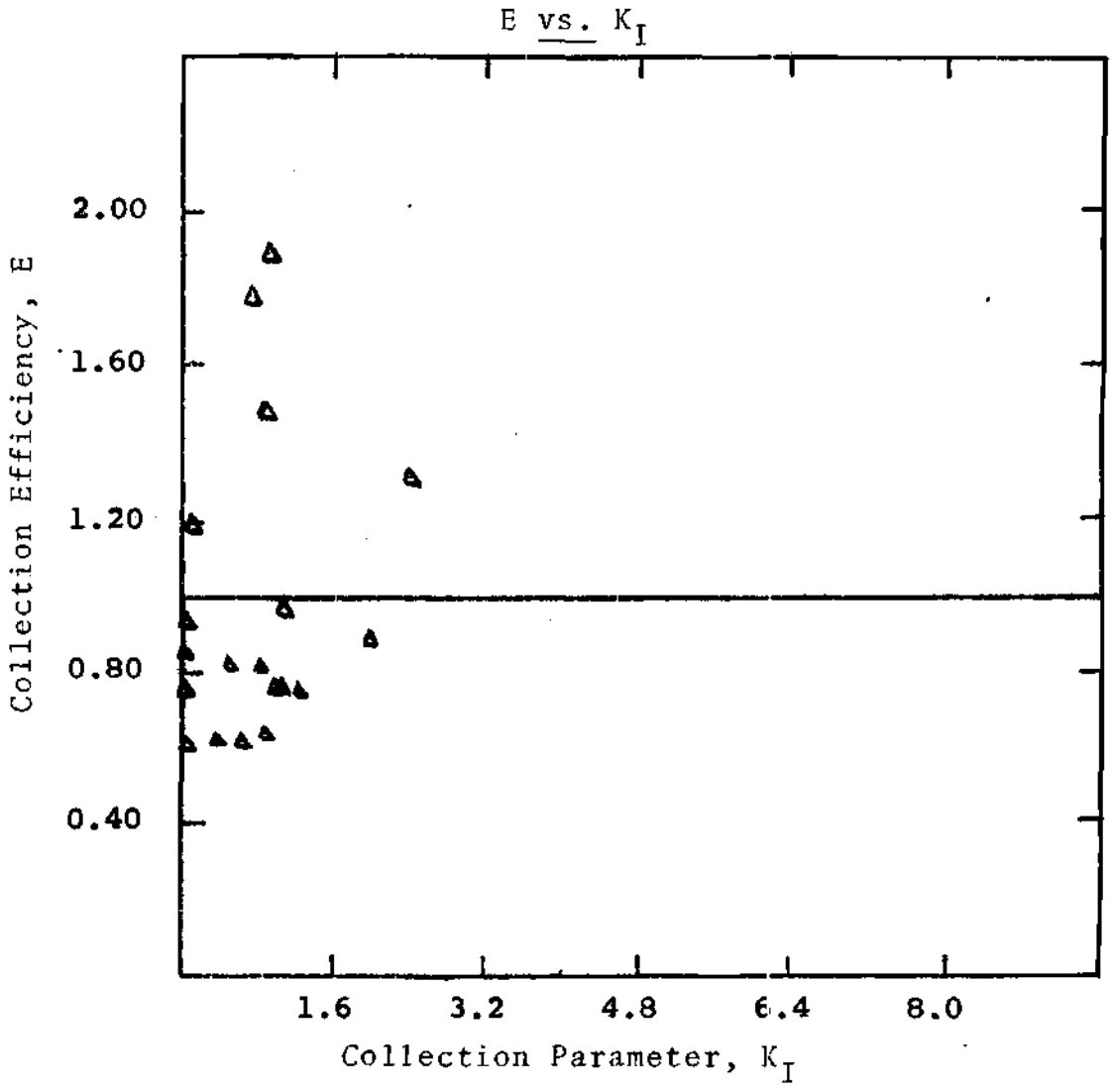

Figure 20. Graph of E vs. K_I for D_p 5.700

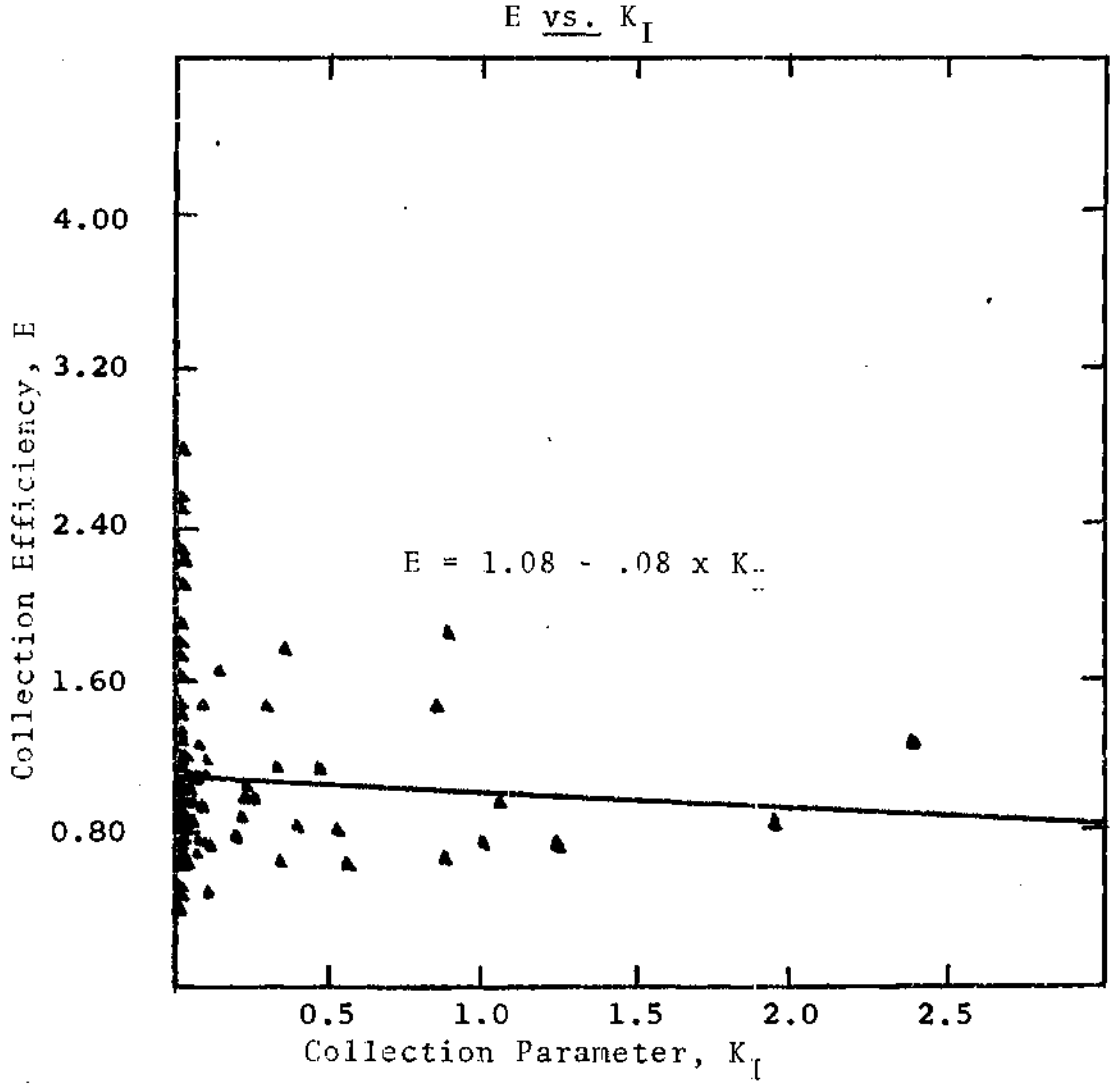

Figure 21. Graph of E vs. K_I for all D_p's

CHAPTER V

CONCLUSIONS

In light of the preceding results, the following conclusions may be drawn:

1. In most cases, there was an increase in collection efficiency with surface charge density; however, after a certain amount of surface charge density, no further changes in collection efficiency were noted.

2. Increasing the surface charge density on water droplets seemed to have a more pronounced effect on the collection of smaller neutral particles in terms of higher amounts of collected aerosol.

3. The collection parameter of Kraemer and Johnstone [18], K_I, may be used to estimate the collection efficiencies of neutral aerosol particles on charged liquid spheres.

CHAPTER VI

RECOMMENDATIONS

The results of this study showed the increased effectiveness of water as a particulate scavenging agent when it carries a surface charge. Additional study is recommended of this phenomenon. To guarantee more reliable data, several improvements should be considered. A better analytical instrument is needed to measure the concentrations of the collected aerosol samples. Using the same particle sizes, tests should be conducted using different flow rates. A check should be made as to the time required for neutralization of aerosol particles by the aerosol neutralizer. A measurement of the charge distribution on the neutralized, monodispersed aerosol should be conducted. Changes should be made in the set-up to assure no deposition of aerosol on the water being collected in the collector. Finally, careful measurements of the important collection parameters and the collection efficiencies should be made, and the theory of Kraemer and Johnstone [18] further tested.

APPENDICES

APPENDIX 1

CALIBRATION OF THE SPECTROPHOTOMETER

The Beckman, Model B, spectrophotometer (see Figure 22) is an accurate, easy-to-operate instrument specifically designed for rapid transmittance and absorbance measurements in the 320 to 1000 millimicrometers spectral range. The Model B consists of a single unit, housing a high gain d-c amplifier, essential optical components, light source, absorption cells, and a photoreceiver. Light from a tungsten lamp is focused by a condensing mirror and directed in a beam to the diagonal entrance mirror. The entrance mirror deflects the light through the entrance slit and into the monochromator to the plane mirror. Light striking the plane mirror is reflected to the Fry prism where it is dispersed into its component wavelengths. The back surface of the prism is aluminized so that light refracted at the first surface and transmitted through the prism is reflected back through the prism undergoing further refraction as it emerges from the prism. The desired wavelength of light is obtained by rotating the wavelength selector which adjusts the position of the prism. The wavelength of light is directed back to the plane mirror where it is reflected through the adjustable exit slit, a lens, and the sample. Light transmitted by the

sample impinges on the phototube causing a current gain which registers on a meter.

The spectrophotometer is equipped with two Beckman pyrex rectangular cells which serve as liquid sample holders. These holders were washed thoroughly with distilled water and dried with tissue paper to prevent any type of foreign material including fingerprints from giving an erroneous spectrophotometer reading. Each rectangular cell was then filled with distilled water, placed in the spectrophotometer, and had its reading recorded. Both cells gave the same reading; therefore, no correction factor was necessary to allow for any discrepancy that would result from use of either cell.

Before the calibration tests could be made, the proper wavelength had to be selected. This selection process entailed making up a couple of solutions from the 1.101 micrometers, 10% solids, Dow uniform latex particles polystrene sample. Each solution used distilled water as its reference at 100% T and was exposed to various wavelengths. From the recorded transmittances, it was observed that the maximum transmittance for each solution occurred around 345 millimicrometers; therefore, this wavelength was used in making all of the calibration curves.

Calibration curves were made from 10% solids samples of Dow uniform latex particles for the following particle diameters and compositions: 0.176 micrometers (polystyrene),

0.312 micrometers (polystyrene), 0.481 micrometers (polystyrene), 0.822 (polystyrene), 1.101 micrometers (polystyrene), 2.020 micrometers (polyvinyltoluene), and 5.700 micrometers (styrene divinylbenzene). Each calibration curve was made in the same manner. One cubic centimeter of the uniform latex particle sample was diluted with 99 cc of distilled water to form a 0.1% solids solution. (This assumes that the density of the latex particles is approximately equal to the density of water.) Using distilled water as a reference at 100% T, a reading of the sample solution was made and recorded. The sample solution was then diluted in half, read on the spectrophotometer, and its transmittance recorded repeatedly until its transmittance eventually reached 100% T.

The recorded transmittances for each particle diameter were plotted on a semi-logarithmic graph and showed a linear relationship between the uniform latex particle concentration and the spectrophotometer reading. These plots are given in Figures 23 to 29 and serve as calibration curves for the spectrophotometer in determining the concentration of uniform latex particles in the experimental distilled water samples.

In addition, the logarithms of the recorded transmittances for each particle diameter were plotted on a graph against the concentration in particles per cubic centimeter and showed a linear relationship between the uniform latex particle concentration and the spectrophotometer reading.

These plots are given in Figures 30 to 36 and serve as supplementary calibration curves for the spectrophotometer in determining the concentration of uniform latex particles in the experimental distilled water samples.

The concentration in particles per cubic centimeter is the ratio of the volume of total particles divided by the volume of a single particle and was obtained from the following expression:

$$\text{concentration (particles/cc)} =$$

$$\frac{6 \times \text{concentration (\% solids by volume)}}{\pi \times (D_p \times 10^{-4})^3}$$

where D_p is the diameter of the aerosol particle and concentration (% solids by volume) is taken from the previous spectrophotometer calibration curves.

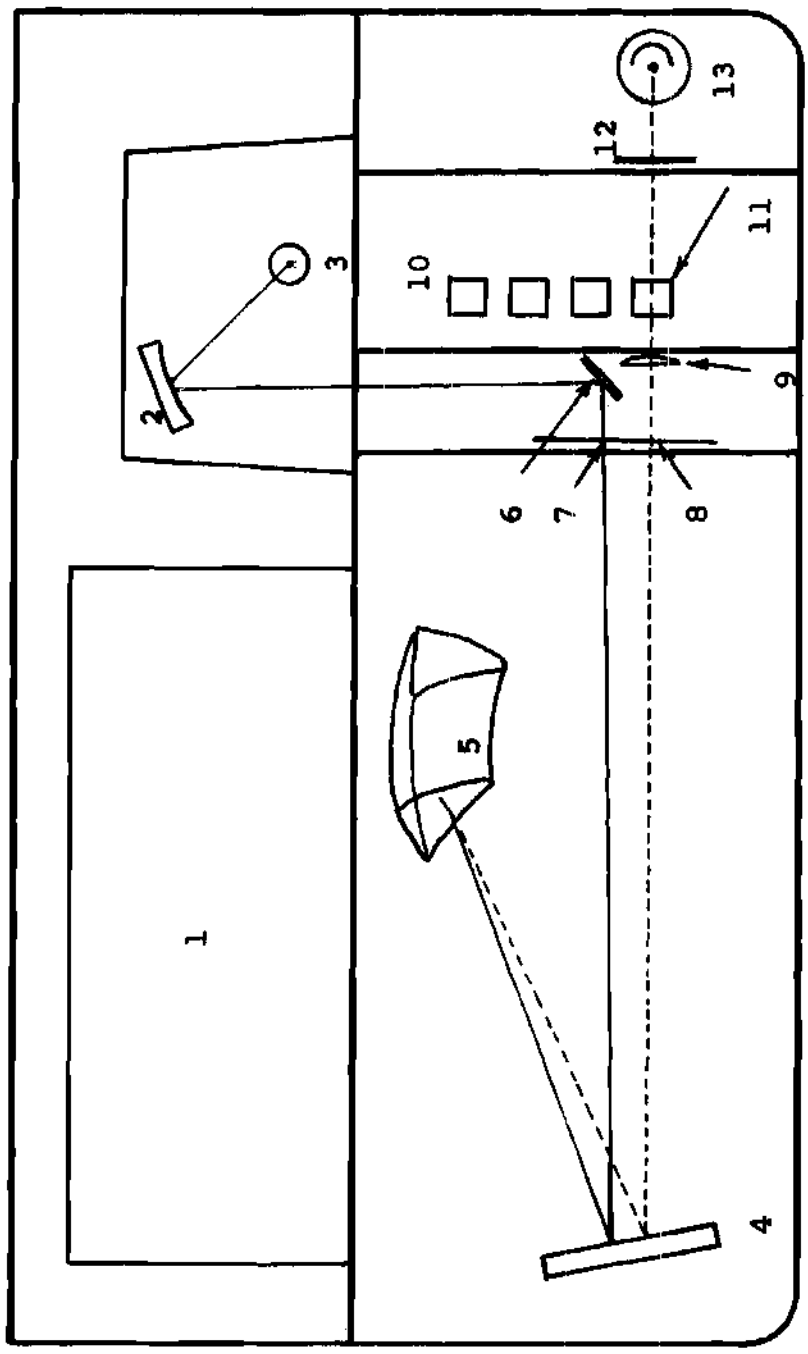

Figure 22. Optical Design of the Spectrophotometer

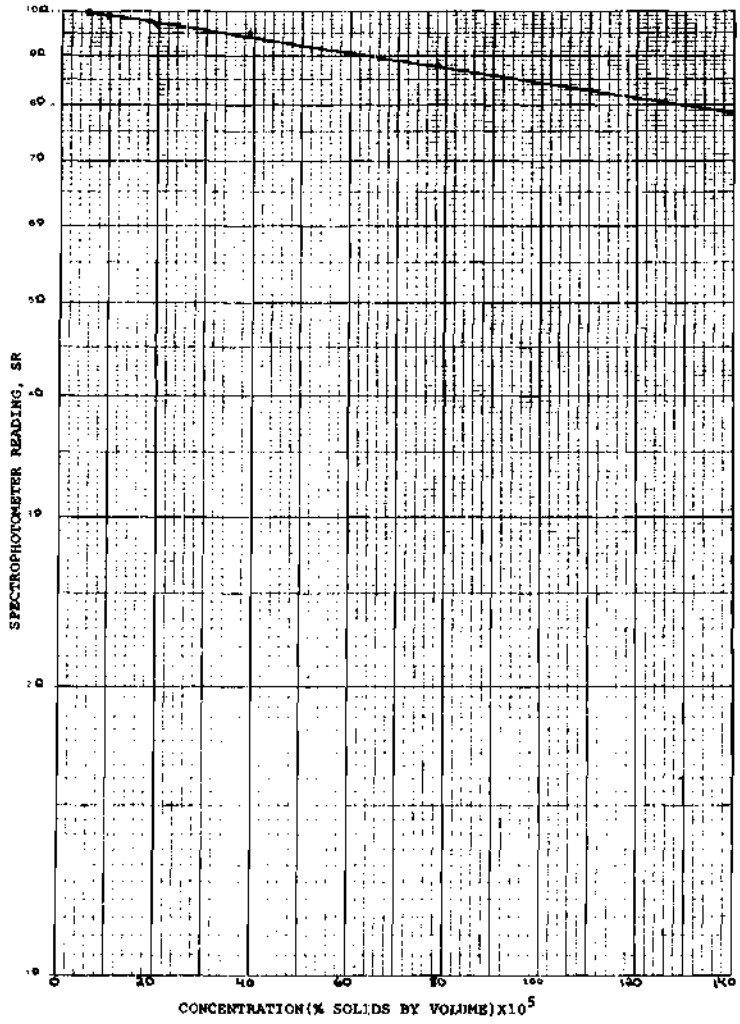

Figure 23. Calibration Curve for the Spectrophotometer, D_p 0.176

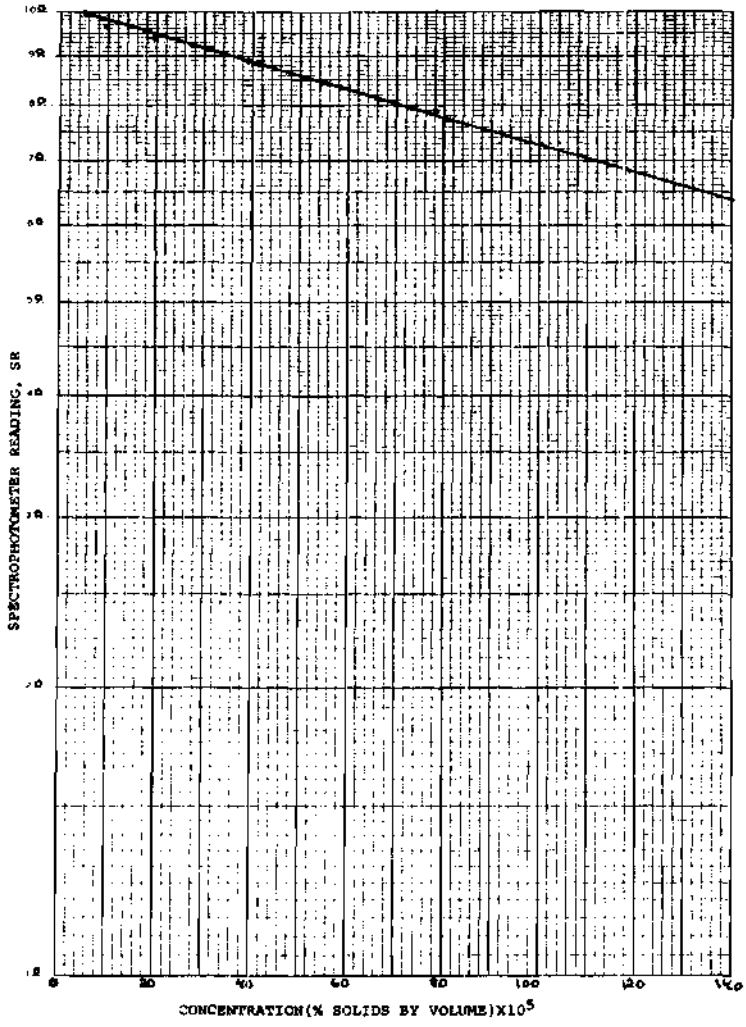

Figure 24. Calibration Curve for the Spectrophotometer, D_p 0.312

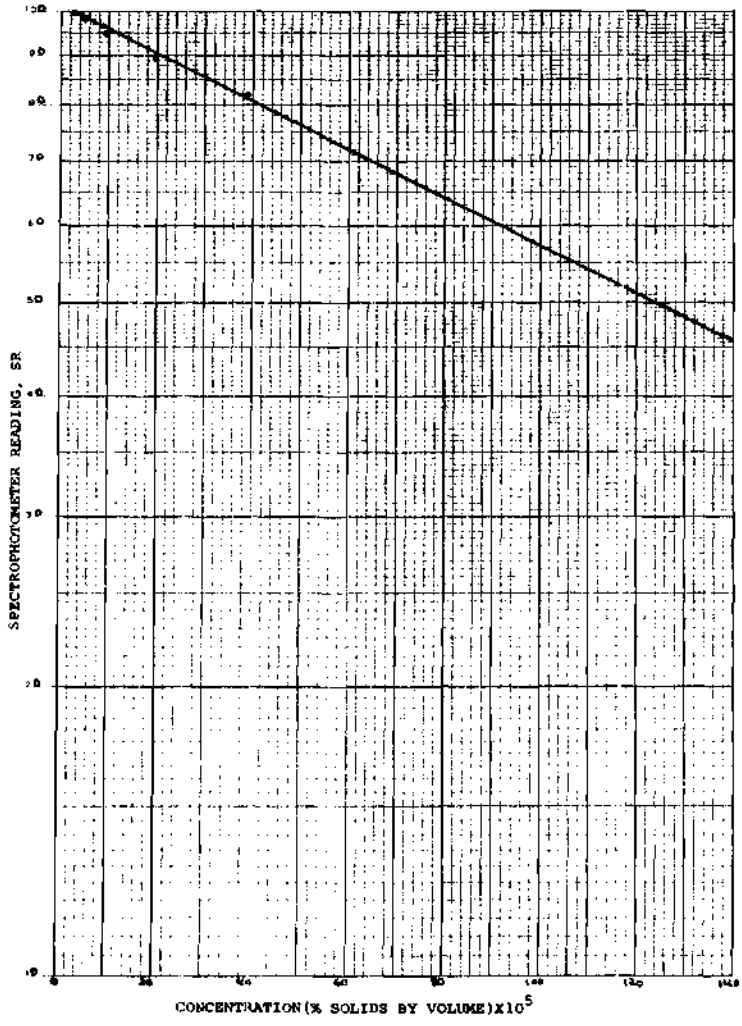

Figure 25. Calibration Curve for the Spectrophotometer, D_p 0.481

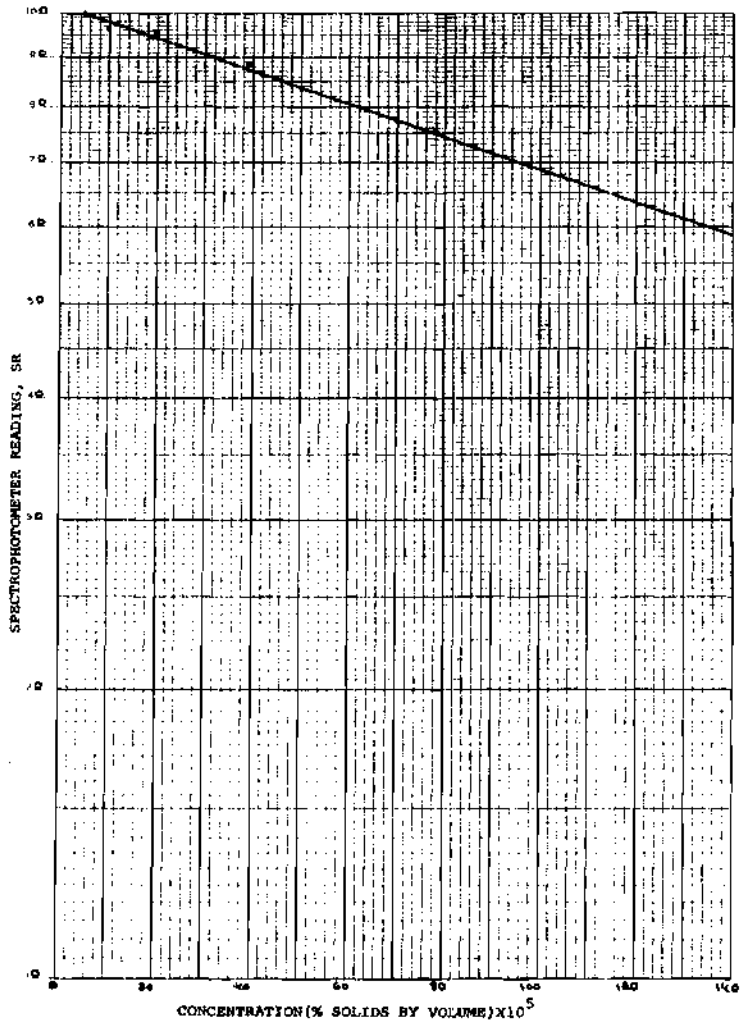

Figure 26. Calibration Curve for the Spectrophotometer, D_p 0.822

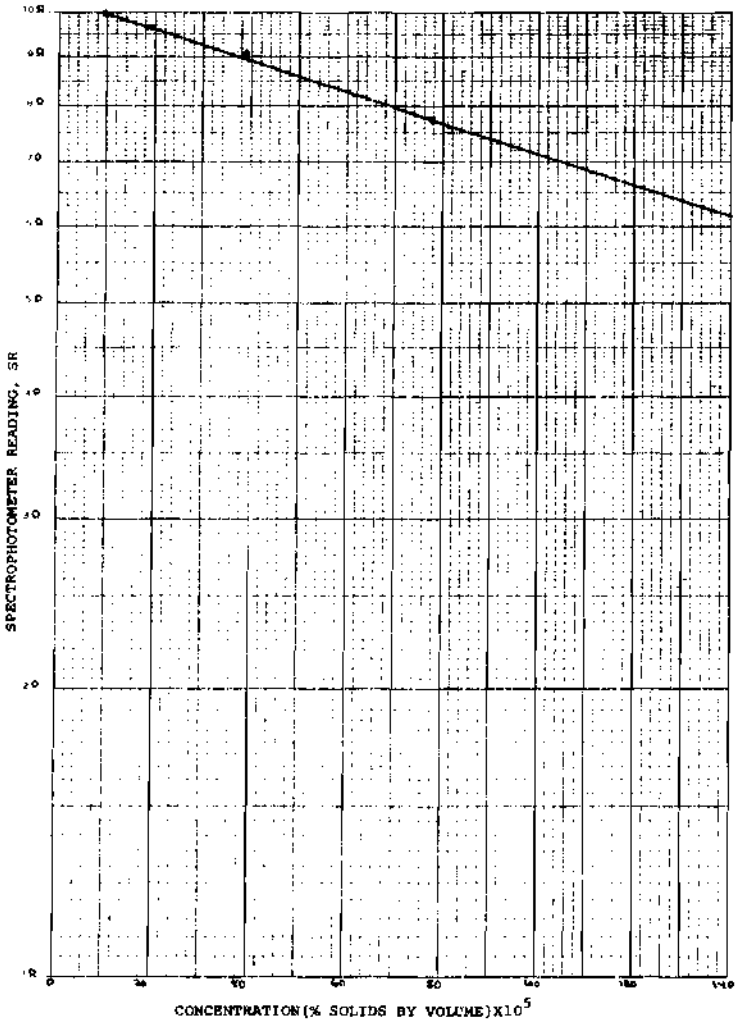

Figure 27. Calibration Curve for the Spectrophotometer, D_p 1.101

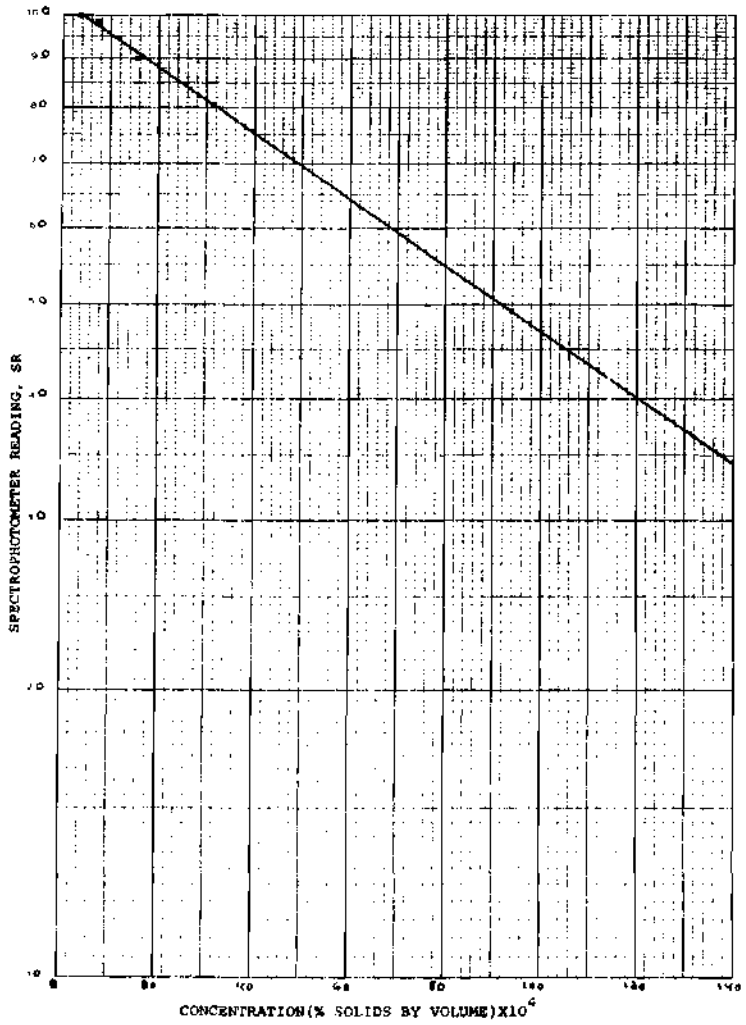

Figure 28. Calibration Curve for the Spectrophotometer, D_p 2.020

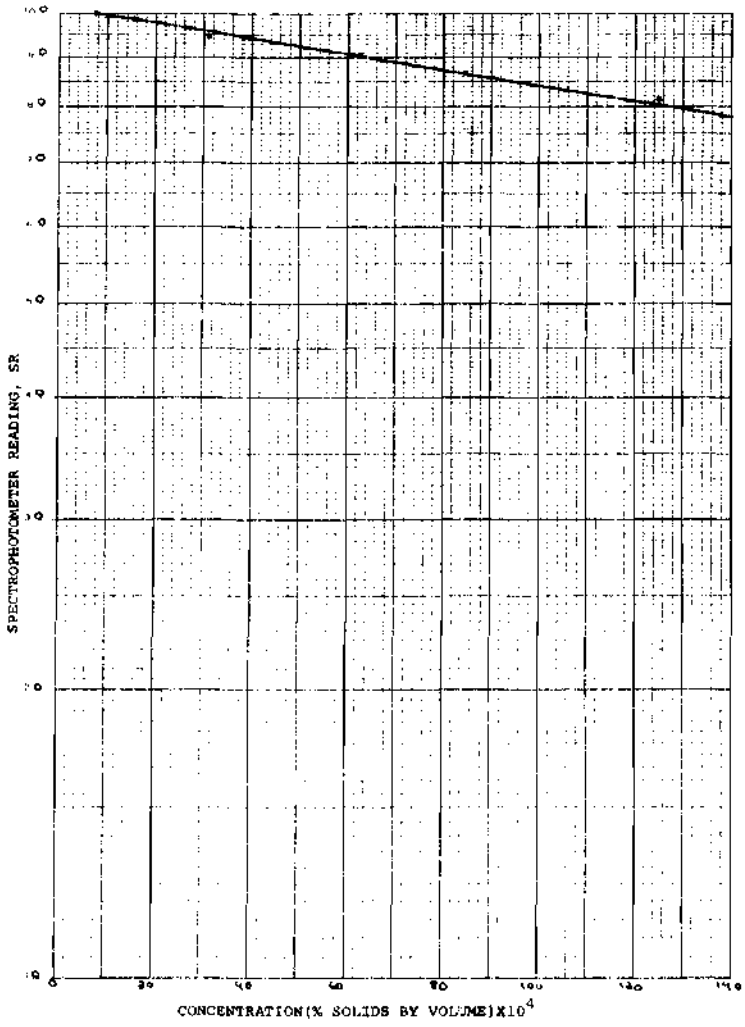

Figure 29. Calibration Curve for the Spectrophotometer, D_p 5.700

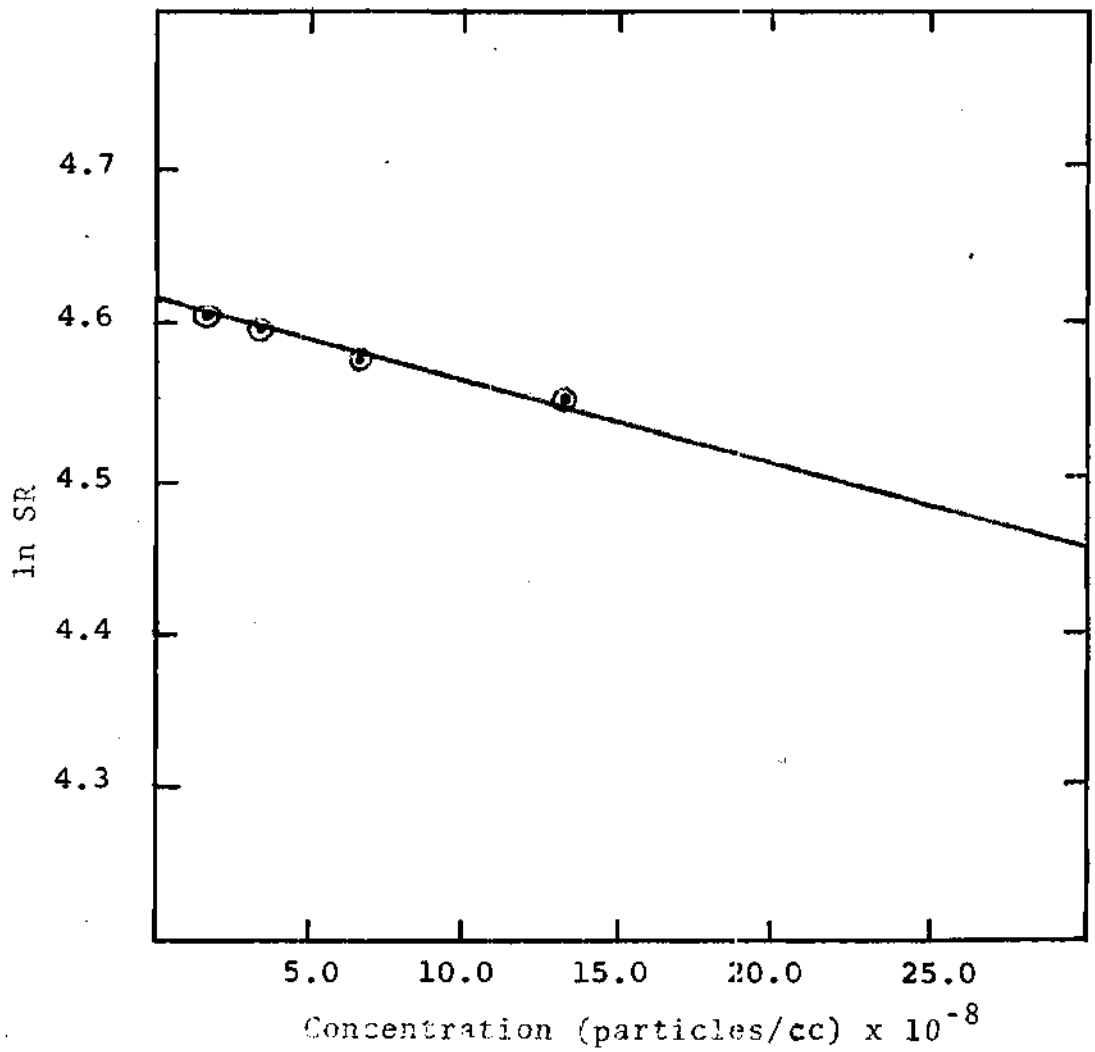

Figure 30. Supplementary Calibration Curve for the Spectrophotometer, D_p 0.176

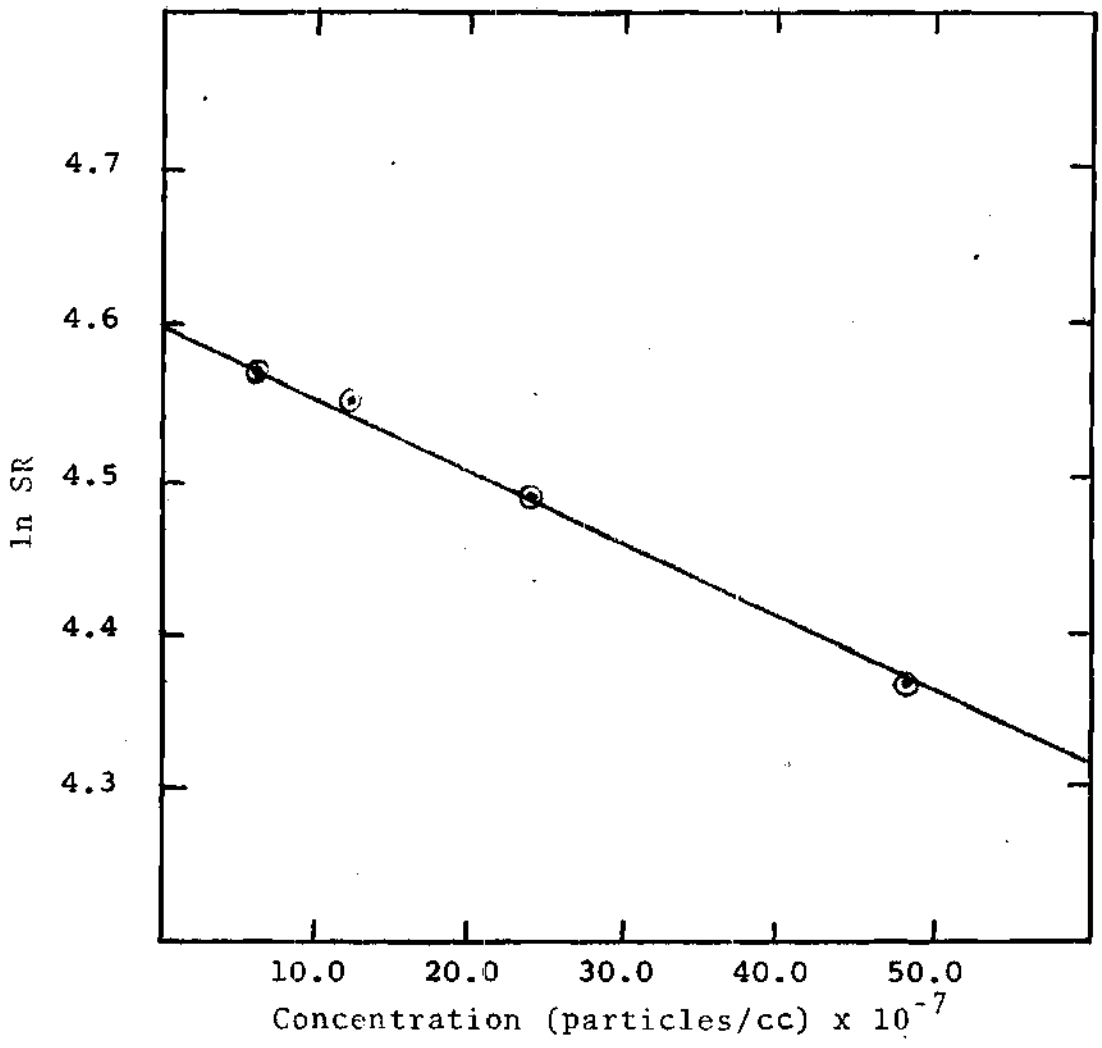

Figure 31. Supplementary Calibration Curve for the Spectrophotometer, D_p 0.312

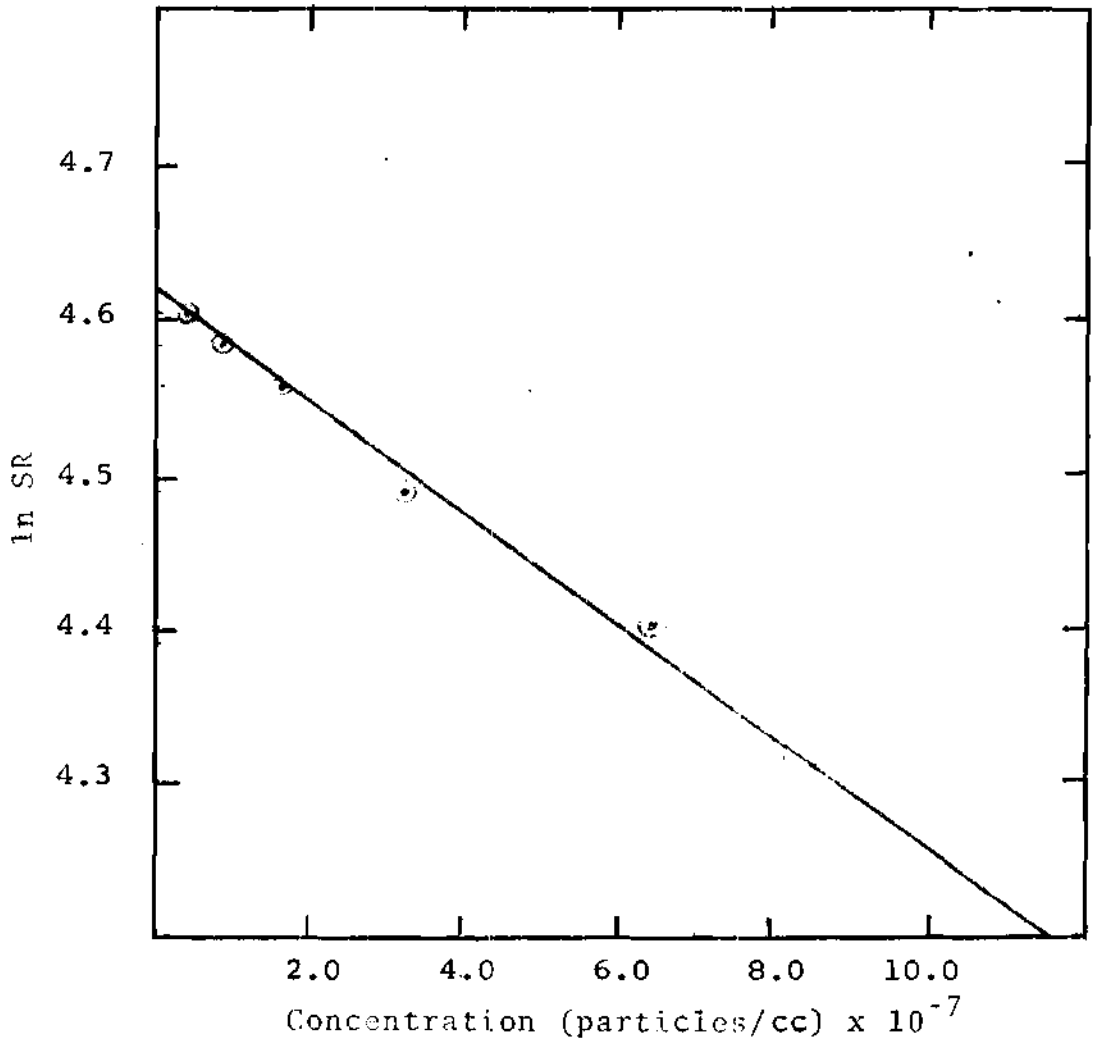

Figure 32. Supplementary Calibration Curve for the Spectrophotometer, D_p 0.481

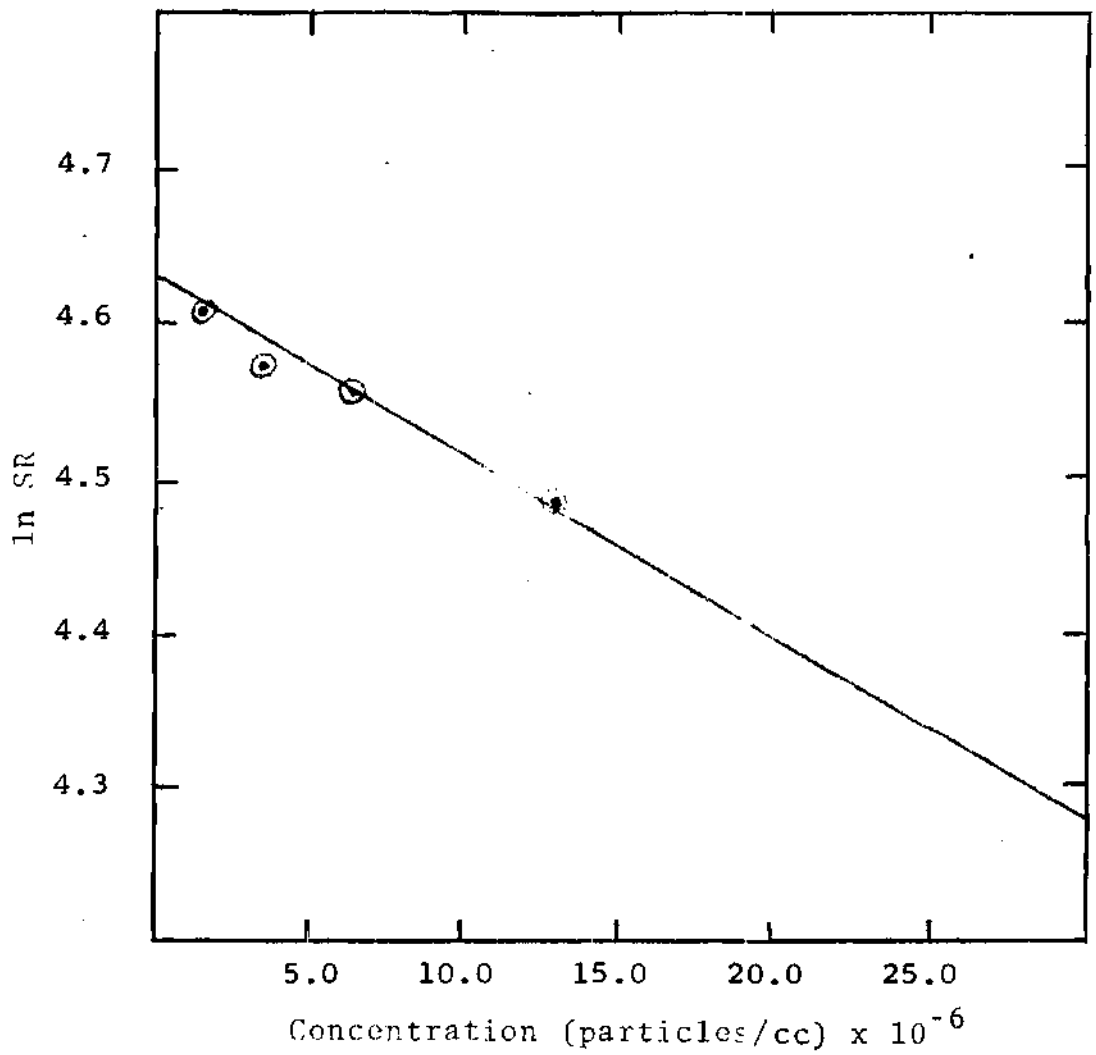

Figure 33. Supplementary Calibration Curve for the Spectrophotometer, D_p 0.822

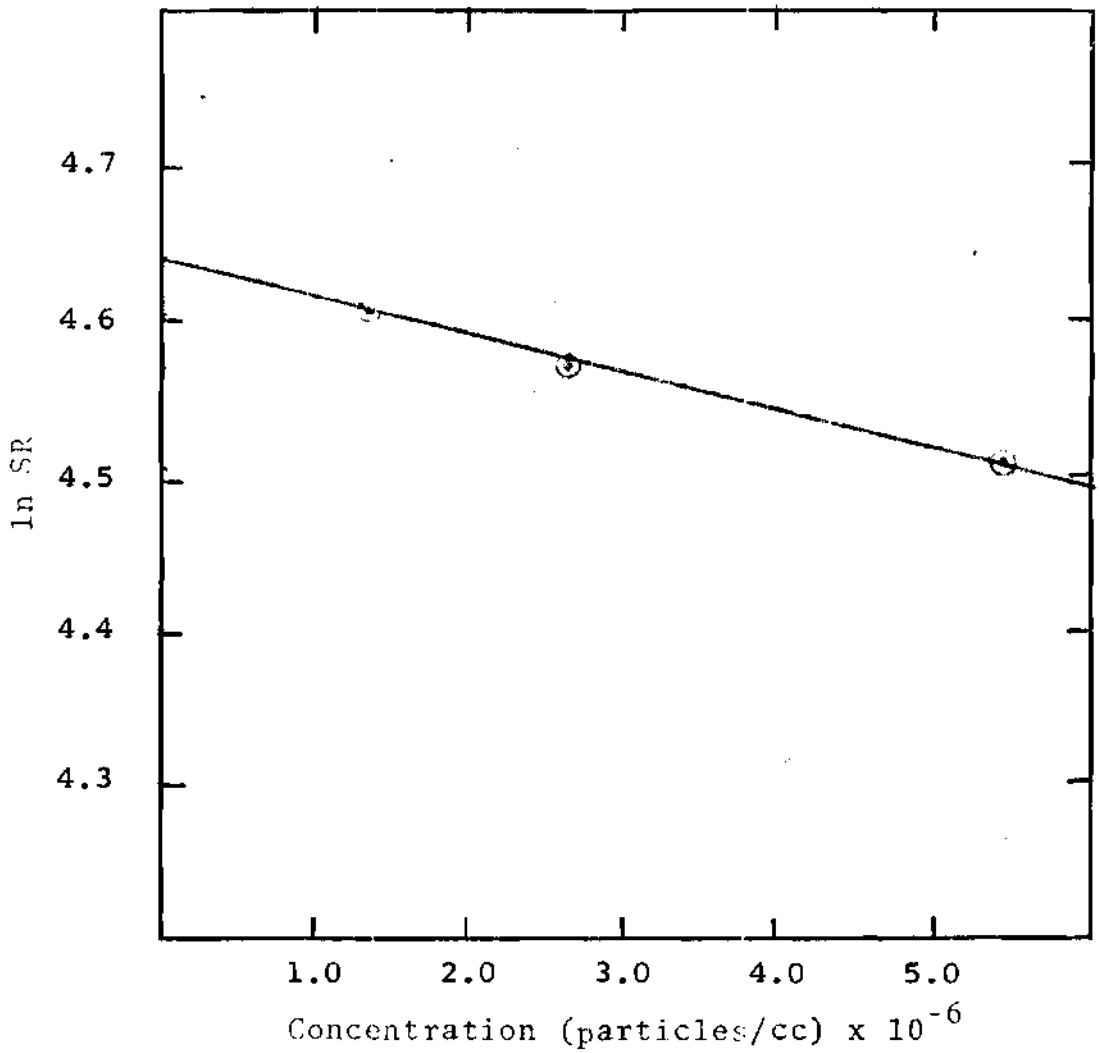

Figure 34. Supplementary Calibration Curve for the Spectrophotometer, D_p 1.101

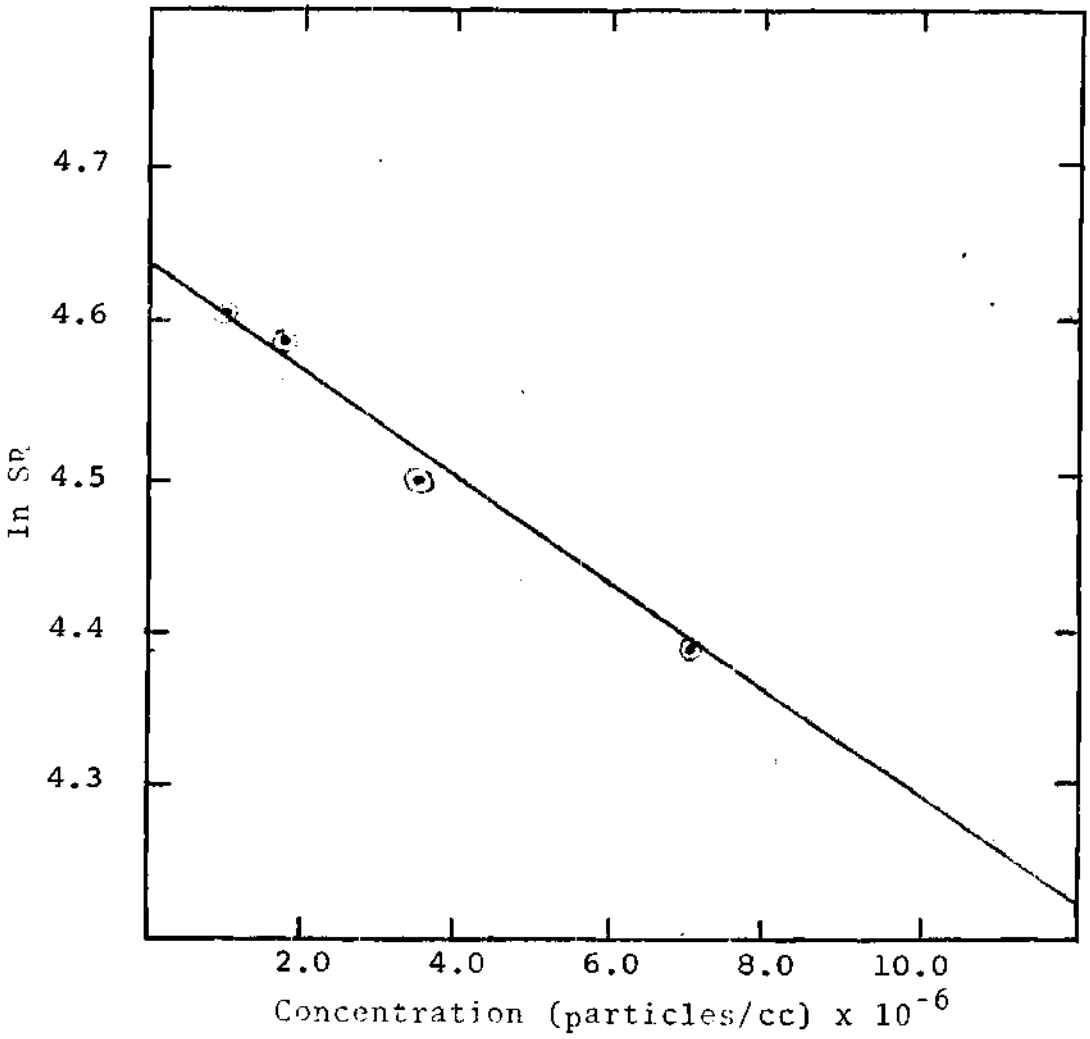

Figure 35. Supplementary Calibration Curve for the Spectrophotometer, D_p 2.020

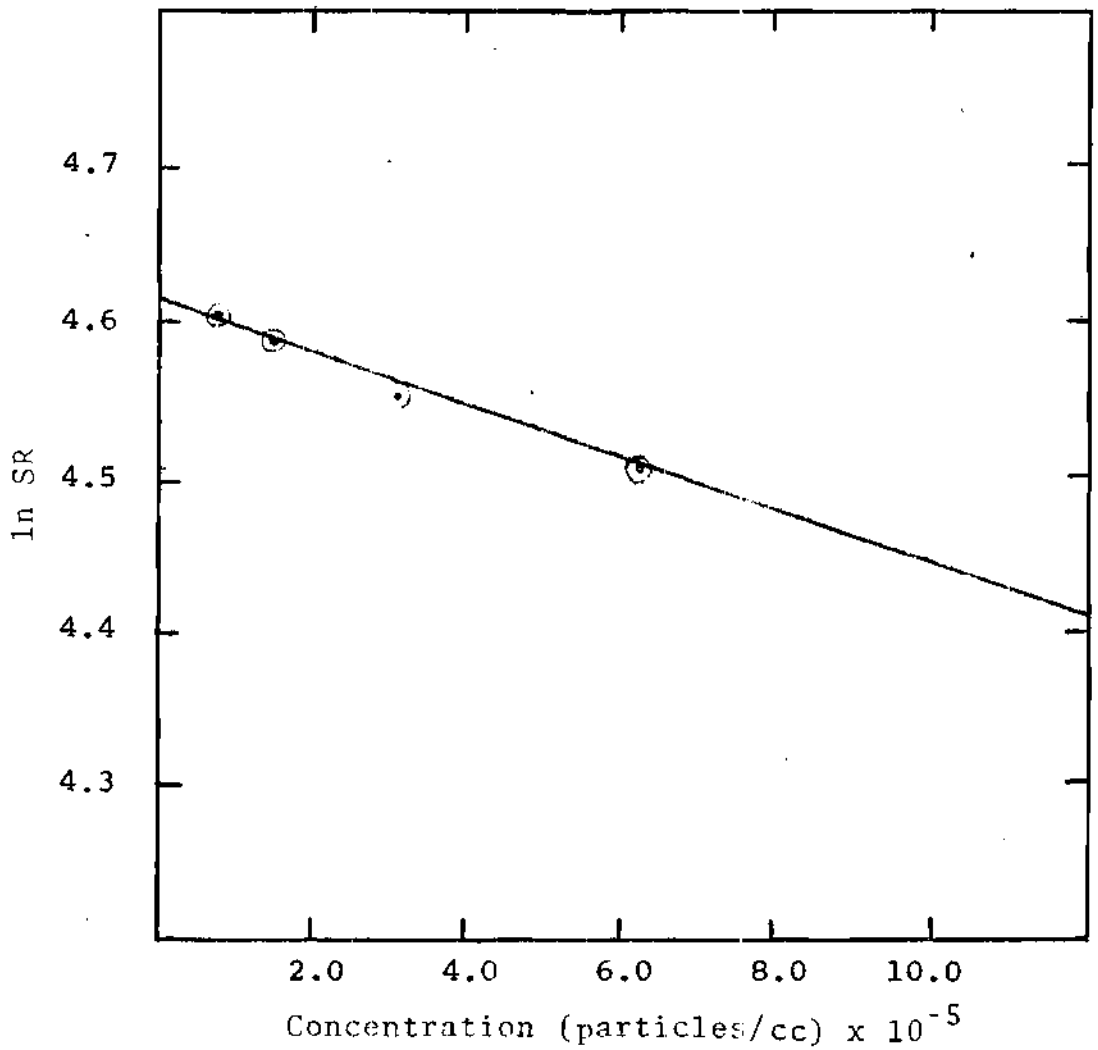

Figure 36. Supplementary Calibration Curve for the Spectrophotometer, D_p 5.700

APPENDIX 2

DERIVATION OF THE CAPACITOR CHARGING CURVE EQUATION

The current, Q_0, now called I_0, was calculated using the voltage and charge relationship for the capacitor, namely,

$$V = Q/C_e = I_1 R_s$$

where R_s is the system resistance and I_1 is the leakage current.

$$\frac{dV}{dt} = \frac{(dQ/dt)}{C_e}$$

$$\frac{dQ}{dt} = I_0 - I_1 = I_0 - V/R_s$$

Separating variables and integrating gives

$$\frac{1}{R_s C_e} \int_{t_0}^{t_c} dt = \int_{V_0}^{V_c} \frac{dV}{I_0 R_s - V}$$

$$- (t_c - t_0)/R_s C_e = \ln(I_0 R_s - V_c) - \ln(I_0 R_s - V_0)$$

Choosing $t_o = V_o = 0$ yields

$$- \frac{tc}{R_s C_e} = \ln \left(\frac{I_0 R_s - V_c}{I_0 R_s}\right) = \ln(1 - Vc/I_0 R_s)$$

$$\exp(-tc/R_s C_e) = 1 - Vc/I_0 R_s$$

and thus

$$I_0 = \frac{Vc}{R_s} \left[1 - \exp\left(- \frac{tc}{R_s C_e}\right)\right]^{-1}$$

Substituting Q_0 for I_0 yields Equation 4

$$Q_0 = \frac{Vc}{R_s} \left[1 - \exp\left(\frac{-tc}{R_s C_e}\right)\right]^{-1}$$

APPENDIX 3

EXPERIMENTALLY MEASURED PARAMETERS

Table 1. Nomenclature

A	cross-sectional area of needle's tip (cm^2)
C	Cunningham factor
C_a	amount of aerosol collected per unit area ($\mu g/cm^2$)
C_e	electrical capacitance (farads)
C_p	amount of aerosol collected per unit area ($particles/cm^2$)
D_p	diameter of aerosol particle (μm)
DR	drop rate (sec^{-1})
ε_o	permittivity of free space = 8.85×10^{-21} $c^2/dyne\text{-}cm^2$
E	collection efficiency
F_a	volumetric flow rate of aerosol stream (cc/min)
F_f	volumetric flow rate of flushing air (cc/min)
F_w	volumetric flow rate of water (cc/min)
K_E	collection parameter for charged aerosol on charged sphere (see page 6)
K_G	collection parameter for charged aerosol on grounded sphere (see page 6)
K_I	collection parameter for uncharged aerosol (Equation 2)
N	viscosity of air (poises)
P	atmospheric pressure (cm Hg)
ρ	density of water (g/cc)
Q	total charge on each droplet (coulombs)
Q_0	current delivered to the capacitor (coulombs/min)
q	surface charge density ($coulombs/cm^2$)
r	radius of aerosol particle (μm)
R	radius of mature water droplet (mm)
R_s	system resistance (ohms)

SR	spectrophotometer reading (% transmittance)
t_c	capacitor charging time (min)
T_w	water temperature (°C)
U_o	aerosol velocity (cm/sec)
V_a	applied voltage (kilovolts)
V_c	voltage across capacitor at time t_c (volts)
V/s	slope of capacitor charging curve (volts/sec)
X_s	dielectric constant of droplet

Table 2. Experimentally Measured Parameters

Run No.	F_w	DR	V_a	V/s	SR	T_w
	D_p = 0.176		F_f = 5,711	F_a = 12,933		
1	.335	.90	0	--	96.5	23
2	.345	.91	+ .53	.0020	97.5	23
3	.340	.73	+1.09	.0073	98.5	23
4	.335	.97	+1.52	.0216	98.0	23
5	.340	1.06	+2.51	.0333	99.0	23
6	.335	.97	+3.03	.0873	97.5	23
7	.330	.96	+3.97	.0566	97.5	23
8	.340	1.03	0	--	99.0	23
9	.340	1.08	+ .52	.0060	100.0	23
10	.330	1.04	+1.51	.0373	98.5	23
11	.330	1.00	+2.50	.0536	99.0	23
12	.330	1.01	+2.96	.0646	99.5	23
13	.330	.97	+3.98	.0526	99.5	23
14	.330	1.02	- .49	.0423	99.8	23
15	.330	1.02	- .49	.0113	99.5	23
16	.330	1.03	-1.48	.0646	99.0	23
17	.330	1.05	-1.44	.0226	100.0	23
18	.340	1.00	-2.50	.1023	99.0	23
19	.340	1.01	-2.49	.0980	99.5	23
20	.340	.99	-3.01	.0816	99.0	23
21	.340	1.05	-3.01	.0800	99.5	23
22	.335	1.07	-4.02	.1100	99.5	23
23	.340	1.12	-4.05	.1363	99.5	23
	D_p = 0.312		F_f = 5,711	F_a = 12,933		
24	.335	1.02	0	--	99.5	23
25	.330	.88	+ .54	.0056	99.2	23
26	.330	.89	+1.54	.0516	99.5	23
27	.335	.90	+2.57	.0433	100.0	23
28	.330	.93	+2.97	.0240	98.0	23
29	.330	.91	+4.02	.0460	97.0	23
30	.330	.87	0	--	99.5	23
31	.330	.85	+ .53	.0185	99.0	23
32	.330	.89	+1.53	.0203	97.5	23
33	.330	.93	+2.53	.0716	97.0	23
34	.340	.92	+3.07	.0730	97.0	23
35	.340	.93	+3.97	.0800	98.0	23
36	.340	.88	0	--	99.5	21
37	.335	.88	- .52	.0260	99.0	21
38	.335	.80	-1.50	.0260	98.0	21
39	.340	.81	-2.52	.0320	97.5	21

Table 2 (continued)

Run No.	F_w	DR	V_a	V/s	SR	T_w
	D_p = 0.312		F_f = 5,711	F_a = 12,933		
40	.340	.79	-2.98	.0413	97.0	21
41	.340	.83	-3.98	.0776	96.5	21
42	.345	.95	0	--	99.0	23
43	.330	.94	- .48	.0300	98.0	23
44	.345	.90	-1.50	.0486	97.0	23
45	.355	.96	-2.48	.0596	96.0	23
46	.330	1.00	-2.95	.0753	95.5	23
47	.350	1.01	-3.95	.0583	95.0	23
	D_p = 0.481		F_f = 5,711	F_a = 12,933		
48	.350	.95	0	--	95.0	23
49	.350	.90	- .50	.0340	95.5	23
50	.335	.92	-1.52	.0516	96.0	23
51	.335	.92	-2.48	.0756	97.0	23
52	.340	.92	-2.99	.1553	95.0	23
53	.335	.95	-4.01	.2390	98.0	23
54	.355	.95	0	--	95.5	23
55	.335	.94	+ .53	.0123	96.0	23
56	.340	.95	+1.50	.0353	98.0	23
57	.330	.86	+2.47	.0440	97.0	23
58	.330	.90	+3.04	.0743	98.0	23
59	.345	.88	+4.00	.0820	96.0	23
60	.345	1.00	0	--	97.0	23
61	.330	.94	+ .50	.0030	95.0	23
62	.335	.87	+1.50	.0065	97.0	23
63	.340	.88	+2.54	.0383	98.0	23
64	.340	.88	+3.05	.0386	98.0	23
65	.340	.91	+4.06	.0610	98.0	23
66	.335	.91	0	--	98.0	21
67	.330	.87	-.54	.0315	97.0	21
68	.340	.90	-1.50	.0440	96.0	21
69	.340	.95	-2.47	.0580	98.0	21
70	.330	.88	-3.05	.0643	96.5	21
71	.340	.96	-3.96	.0826	96.5	21
	D_p = 0.822		F_f = 5,711	F_a = 12,933		
72	.330	.91	0	--	96.0	24
73	.330	.83	- .53	.0226	98.0	24
74	.330	.85	-1.54	.0436	96.0	24
75	.330	.83	-2.49	.0460	97.0	24
76	.330	.88	-3.04	.0446	96.0	24

Table 2 (continued)

Run No.	F_w	DR	V_a	V/s	SR	T_w
	D_p = 0.822		F_f = 5,711	F_a = 12,933		
77	.330	.89	-3.97	.0656	98.0	24
78	.340	.88	0	--	98.0	24
79	.345	.89	- .50	.0126	96.0	24
80	.345	.83	-1.47	.0126	96.5	23
81	.340	.87	-2.51	.0380	98.0	23
82	.340	.84	-3.04	.0620	97.0	23
83	.340	.87	-4.00	.0463	95.0	23
84	.335	.93	0	--	97.0	23
85	.340	.99	+ .56	.0610	96.5	23
86	.350	.96	+1.50	.0973	97.0	23
87	.350	.90	+2.55	.0960	98.0	23
88	.350	.91	+3.06	.0820	96.5	23
89	.350	.93	+3.99	.0680	97.0	23
90	.350	.90	0	--	97.0	23
91	.350	.93	+ .57	.0650	98.0	23
92	.350	.90	+1.51	.0790	98.0	23
93	.330	.91	+2.47	.0730	97.0	23
94	.355	.85	+3.07	.0540	96.0	23
95	.330	.89	+4.00	.0260	95.0	23
	D_p = 1.101		F_f = 5,711	F_a = 12,933		
96	.355	.94	0	--	94.0	22
97	.335	.95	+ .47	.0105	97.0	22
98	.340	.95	+1.56	.0136	98.0	22
99	.340	1.01	+2.54	.0620	93.5	22
100	.335	.98	+2.97	.0573	98.0	22
101	.340	.94	+3.98	.0645	94.0	22
102	.340	.95	0	--	96.0	22
103	.330	.91	+ .57	.0090	96.0	22
104	.315	.94	+1.49	.0213	94.0	22
105	.335	.93	+2.54	.0285	94.0	22
106	.335	.96	+2.99	.0500	93.5	22
107	.355	.94	+4.01	.0685	97.0	22
108	.340	.97	0	--	95.5	23
109	.355	1.02	- .52	.0120	97.0	23
110	.350	1.00	-1.51	.0336	97.0	23
111	.340	.98	-2.46	.0746	94.0	23
112	.340	.99	-2.98	.0966	96.0	23
113	.355	1.02	-4.00	.1820	95.0	23
114	.330	.99	0	--	95.0	23
115	.355	1.02	- .51	.0203	94.5	23
116	.355	1.02	-1.56	.1010	94.5	23

Table 2 (continued)

Run No.	F_w	DR	V_a	V/s	SR	T_w
	D_p = 1.101		F_f = 5,711	F_a = 12,933		
117	.340	1.00	-2.48	.1605	96.0	23
118	.355	1.02	-2.97	.2165	94.0	23
119	.355	1.00	-3.99	.2565	94.0	23
	D_p = 2.020		F_f = 5,711	F_a = 12,933		
120	.335	.78	0	--	94.0	24
121	.350	.78	- .52	.0086	94.5	24
122	.355	.79	-1.50	.0373	95.0	24
123	.355	.78	-2.55	.0550	96.0	24
124	.350	.81	-3.00	.0553	96.5	24
125	.345	.79	-4.05	.0890	94.0	24
126	.365	.86	0	--	96.5	24
127	.330	.82	- .48	.0106	94.5	24
128	.330	.81	-1.52	.0456	96.0	24
129	.320	.82	-2.55	.0600	98.0	24
130	.330	.84	-2.98	.0586	96.0	24
131	.320	.81	-4.07	.0956	94.0	24
132	.310	.81	0	--	97.0	24
133	.350	.91	+ .49	.0033	96.0	24
134	.335	.91	+1.49	.0200	95.0	24
135	.340	.93	+2.55	.0540	94.0	24
136	.340	.91	+2.99	.0506	95.0	24
137	.355	.92	+4.00	.0753	93.0	24
138	.335	.94	0	--	97.0	24
139	.340	.95	+ .52	.0100	97.0	24
140	.340	.93	+1.50	.0330	98.0	24
141	.340	.94	+2.50	.0553	98.0	24
142	.345	.94	+2.99	.0853	98.0	24
143	.340	.93	+3.99	.0973	97.0	24
	D_p = 5.700		F_f = 5,711	F_a = 12,933		
144	.360	.81	0	--	93.0	22
145	.350	.82	+ .53	.0060	95.0	22
146	.350	.84	+1.55	.0220	95.0	22
147	.365	.85	+2.52	.0443	96.0	22
148	.365	.85	+3.02	.0750	95.0	22
149	.365	.86	+4.00	.0830	96.0	22
150	.300	.71	0	--	93.0	22
151	.355	.83	+ .50	.0190	93.5	22
152	.365	.87	+1.52	.0180	94.0	22
153	.365	.88	+2.49	.0476	94.5	22

Table 2 (concluded)

Run No.	F_w	DR	V_a	V/s	SR	T_w
	D_p = 5.700		F_f = 5,711	F_a = 12,933		
154	.365	.86	+2.97	.0713	96.0	22
155	.365	.88	+3.99	.0573	96.0	22
156	.365	.81	0	--	94.0	23
157	.355	.79	- .47	.0166	97.0	23
158	.370	.81	-1.55	.0543	95.5	23
159	.370	.83	-2.55	.0780	94.5	23
160	.370	.85	-3.06	.1063	95.0	23
161	.370	.85	-3.98	.1426	97.0	23
162	.350	.87	0	--	96.0	21
163	.370	.91	- .49	.0253	95.0	21
164	.370	.92	-1.48	.0440	92.0	21
165	.370	.90	-2.53	.0726	91.5	21
166	.380	.91	-3.00	.0736	93.5	21
167	.380	.93	-4.07	.1243	94.5	21

APPENDIX 4

CALCULATED PARAMETERS

Table 3. Calculated Parameters

Run No.	R	$Q_o x10^{10}$	$qx10^{11}$	q^2x10^{22}	C	U_o	K_I	C_a	E
1	1.139	--	--	--	2.02	11.01	--	.0907	1.0
2	1.146	.095	6.324	40	2.02	11.34	$1.53x10^{-6}$	.0684	.75
3	1.225	.348	25.188	634	2.02	11.18	$2.30x10^{-5}$	.0489	.54
4	1.111	1.030	68.437	4,684	2.02	11.01	$1.90x10^{-4}$	.0590	.65
5	1.082	1.588	101.480	10,298	2.02	11.18	$4.22x10^{-4}$	.0358	.39
6	1.109	4.164	276.672	76,547	2.02	11.01	$3.11x10^{-3}$	.0662	.73
7	1.109	2.699	181.869	33,076	2.02	10.85	$1.37x10^{-3}$	.0662	.73
8	1.094	--	--	--	2.02	11.18	--	.0362	1.0
9	1.075	.286	18.165	330	2.02	11.18	$1.36x10^{-5}$	.0179	.49
10	1.080	1.779	116.751	13,630	2.02	10.85	$5.78x10^{-4}$	.0429	1.18
11	1.094	2.556	169.915	28,871	2.02	10.85	$1.21x10^{-3}$	.0363	1.00
12	1.090	3.081	204.058	41,639	2.02	10.85	$1.75x10^{-3}$	.0253	.70
13	1.105	2.509	168.359	28,345	2.02	10.85	$1.17x10^{-3}$	.0255	.70
14	1.087	2.017	133.111	17,719	2.02	10.85	$7.48x10^{-4}$	.0180	.50
15	1.087	.548	36.164	1,308	2.02	10.85	$5.51x10^{-5}$	.0251	.69
16	1.084	3.081	202.623	41,056	2.02	10.85	$1.73x10^{-3}$	.0358	.99
17	1.076	1.078	70.518	4,973	2.02	10.85	$2.12x10^{-4}$	.0178	.49
18	1.105	4.879	317.960	101,099	2.02	11.18	$4.07x10^{-3}$	.0366	1.01
19	1.101	4.674	303.457	92,086	2.02	11.18	$3.72x10^{-3}$	.0255	.70
20	1.109	3.892	254.312	64,674	2.02	11.18	$2.59x10^{-3}$	.0366	1.01

Table 3 (continued)

Run No.	R	$Q_o x10^{11}$	$qx10^{11}$	q^2x10^{22}	C	U_o	K_I	C_a	E
21	1.087	3.816	244.638	59,848	2.02	11.18	$2.45x10^{-3}$	.0251	.69
22	1.075	5.247	337.680	114,027	2.02	11.01	$4.79x10^{-3}$	.0248	.69
23	1.064	6.501	407.951	166,425	2.02	11.18	$6.94x10^{-3}$	.0246	.68
24	1.093	--	--	--	1.55	11.01	--	.0217	1.00
25	1.142	.267	18.515	342	1.55	10.85	$3.32x10^{-5}$	.0264	1.22
26	1.138	2.461	169.977	28,892	1.55	10.85	$2.80x10^{-3}$	.0225	1.04
27	1.139	2.065	140.701	19,797	1.55	11.01	$1.89x10^{-3}$	.0189	.87
28	1.121	1.144	77.840	6,059	1.55	10.85	$5.97x10^{-4}$	.0371	1.71
29	1.129	2.194	150.543	22,663	1.55	10.85	$2.22x10^{-3}$	.0487	2.25
30	1.146	--	--	--	1.55	10.85	--	.0227	1.00
31	1.155	.882	61.839	3,824	1.55	10.85	$3.65x10^{-4}$	.0268	1.18
32	1.138	.968	66.858	4,470	1.55	10.85	$4.34x10^{-4}$	.0414	1.82
33	1.121	3.415	232.366	53,994	1.55	10.85	$5.31x10^{-3}$	.0482	2.12
34	1.136	3.482	233.211	54,387	1.55	11.18	$5.12x10^{-3}$	.0489	2.15
35	1.132	3.816	254.664	64,854	1.55	11.18	$6.14x10^{-3}$	.0375	1.65
36	1.153	--	--	--	1.55	11.18	--	.0229	1.00
37	1.147	1.240	85.180	7,256	1.55	11.01	$6.88x10^{-4}$	.0266	1.16
38	1.185	1.240	87.856	7,719	1.55	11.01	$7.08x10^{-4}$	.0392	1.71
39	1.185	1.526	106.661	11,377	1.55	11.18	$1.02x10^{-3}$	.0433	1.89
40	1.196	1.970	138.773	19,258	1.55	11.18	$1.73x10^{-3}$	.0515	2.24

Table 3 (continued)

Run No.	R	$Q_o x10^{10}$	$qx10^{11}$	q^2x10^{22}	C	U_o	K_I	C_a	E
41	1.176	3.701	256.571	65,829	1.55	11.18	$5.99x10^{-3}$	.0586	2.55
42	1.129	--	--	--	1.55	11.34	--	.0262	1.00
43	1.117	1.431	97.038	9,417	1.55	10.85	$9.30x10^{-4}$	.0369	1.41
44	1.150	2.318	154.956	24,012	1.55	11.34	$2.20x10^{-3}$	.0496	1.89
45	1.136	2.842	182.414	33,275	1.55	11.67	$3.01x10^{-3}$	.0602	2.30
46	1.094	3.591	238.719	56,987	1.55	10.85	$5.75x10^{-3}$	.0654	2.50
47	1.112	2.780	176.962	31,316	1.55	11.51	$2.93x10^{-3}$	.0738	2.82
48	1.135	--	--	--	1.35	11.51	--	.0450	1.00
49	1.155	1.621	107.339	11,522	1.35	11.51	$2.15x10^{-3}$	.0421	.93
50	1.131	2.461	166.424	27,697	1.35	11.01	$5.52x10^{-3}$	.0375	.83
51	1.131	3.606	243.855	59,465	1.35	11.01	$1.19x10^{-2}$	.0300	.67
52	1.136	7.407	496.095	246,111	1.35	11.18	$4.80x10^{-2}$	.0453	1.00
53	1.118	11.400	763.066	582,270	1.35	11.01	$1.17x10^{-1}$	.0221	.49
54	1.118	--	--	--	1.35	11.67	--	.0431	1.00
55	1.123	.586	39.352	1,549	1.35	11.01	$3.10x10^{-4}$	.0371	.86
56	1.124	1.683	111.559	12,446	1.35	11.18	$2.45x10^{-3}$	.0223	.52
57	1.151	2.098	146.597	21,490	1.35	10.85	$4.27x10^{-3}$	.0305	.71
58	1.133	3.544	243.808	59,442	1.35	10.85	$1.20x10^{-2}$	.0225	.52
59	1.159	3.911	263.310	69,333	1.35	11.34	$1.31x10^{-2}$	.0384	.89
60	1.110	--	--	--	1.35	11.34	--	.0294	1.00

Table 3 (continued)

Run No.	R	$Q_o x10^{10}$	$qx10^{11}$	q^2x10^{22}	C	U_o	K_I	C_a	E
61	1.117	.143	9.695	94	1.35	10.85	$1.92x10^{-5}$	.0444	1.51
62	1.152	.310	21.360	456	1.35	11.01	$8.90x10^{-5}$	.0305	1.04
63	1.153	1.826	124.102	15,401	1.35	11.18	$2.96x10^{-3}$	.0230	.78
64	1.153	1.841	125.121	15,655	1.35	11.18	$3.01x10^{-3}$	.0230	.78
65	1.140	2.909	195.562	38,245	1.35	11.18	$7.42x10^{-3}$	.0225	.77
66	1.135	--	--	--	1.35	11.01	--	.0225	1.00
67	1.146	1.502	104.612	10,944	1.35	10.85	$2.18x10^{-3}$	.0305	1.35
68	1.144	2.098	141.590	20,048	1.35	11.18	$3.88x10^{-3}$	.0380	1.69
69	1.124	2.766	183.350	33,617	1.35	11.18	$6.63x10^{-3}$	.0223	.99
70	1.142	3.067	212.704	45,243	1.35	10.85	$9.03x10^{-3}$	.0341	1.51
71	1.120	3.940	260.343	67,779	1.35	11.18	$1.34x10^{-2}$	.0334	1.49
72	1.129	--	--	--	1.21	10.85	--	.0562	1.00
73	1.164	1.078	76.227	5,811	1.21	10.85	$2.99x10^{-3}$	.0386	.69
74	1.153	2.079	146.284	21,399	1.21	10.85	$1.11x10^{-2}$	.0577	1.03
75	1.164	2.194	155.145	24,070	1.21	10.85	$1.23x10^{-2}$	.0463	.82
76	1.142	2.127	147.513	21,760	1.21	10.85	$1.14x10^{-2}$	.0569	1.01
77	1.138	3.129	216.114	46,705	1.21	10.85	$2.45x10^{-2}$	.0377	.67
78	1.153	--	--	--	1.21	11.18	--	.0381	1.00
79	1.155	1.030	69.052	4,768	1.21	11.34	$2.37x10^{-3}$	.0574	1.51
80	1.182	1.030	70.664	4,993	1.21	11.34	$2.42x10^{-3}$	.0508	1.33

Table 3 (continued)

Run No.	R	$Q_o x10^{10}$	$qx10^{11}$	$q^2 x10^{22}$	C	U_o	K_I	C_a	E
81	1.157	1.812	123.685	15,298	1.21	11.18	$7.69x10^{-3}$	.0384	1.01
82	1.171	2.957	204.208	41,701	1.21	11.18	$2.07x10^{-2}$	.0466	1.22
83	1.157	2.208	150.717	22,716	1.21	11.18	$1.14x10^{-2}$	.0691	1.81
84	1.127	--	--	--	1.21	11.01	--	.0448	1.00
85	1.109	2.909	190.080	36,131	1.21	11.18	$1.89x10^{-2}$	.0478	1.07
86	1.131	4.641	300.769	90,462	1.21	11.51	$4.51x10^{-2}$	.0450	1.00
87	1.155	4.579	303.217	91,941	1.21	11.51	$4.48x10^{-2}$	.0384	.86
88	1.151	3.911	257.962	66,544	1.21	11.51	$3.26x10^{-2}$	.0496	1.11
89	1.143	3.243	212.310	45,076	1.21	11.51	$2.23x10^{-2}$	.0455	1.01
90	1.155	--	--	--	1.21	11.51	--	.0459	1.00
91	1.143	3.100	202.949	41,188	1.21	11.51	$2.03x10^{-2}$	.0380	.83
92	1.155	3.768	249.513	62,257	1.21	11.51	$3.04x10^{-2}$	.0384	.84
93	1.129	3.482	238.920	57,083	1.21	10.85	$3.03x10^{-2}$	.0448	.98
94	1.183	2.575	172.105	29,620	1.21	11.67	$1.39x10^{-2}$	.0590	1.29
95	1.138	1.240	85.644	7,335	1.21	10.85	$3.86x10^{-3}$	.0680	1.48
96	1.144	--	--	--	1.15	11.67	--	.0950	1.00
97	1.118	.500	33.467	1,120	1.15	11.01	$1.00x10^{-3}$	.0631	.66
98	1.124	.648	42.952	1,845	1.15	11.18	$1.62x10^{-3}$	.0521	.55
99	1.101	2.957	191.981	36,857	1.15	11.18	$3.31x10^{-2}$	.0987	1.04
100	1.107	2.733	181.071	32,787	1.15	11.01	$2.98x10^{-2}$	.0515	.54

Table 3 (continued)

Run No.	R	$Q_o \times 10^{10}$	$q \times 10^{11}$	$q^2 \times 10^{22}$	C	U_o	K_I	C_a	E
101	1.128	3.076	204.573	41,850	1.15	11.18	3.67×10^{-2}	.0935	.98
102	1.124	--	--	--	1.15	11.18	--	.0747	1.00
103	1.129	.429	29.436	866	1.15	10.85	7.82×10^{-4}	.0751	1.01
104	1.099	1.016	71.138	5,061	1.15	10.36	4.92×10^{-3}	.0914	1.22
105	1.127	1.359	91.574	8,386	1.15	11.01	7.48×10^{-3}	.0935	1.25
106	1.114	2.385	159.140	25,326	1.15	11.01	2.23×10^{-2}	.1000	1.34
107	1.144	3.267	211.102	44,564	1.15	11.67	3.69×10^{-2}	.0646	.86
108	1.116	--	--	--	1.15	11.18	--	.0780	1.00
109	1.114	.572	35.965	1,293	1.15	11.67	1.10×10^{-3}	.0629	.81
110	1.116	1.602	102.368	10,479	1.15	11.51	9.03x10-3	.0629	.81
111	1.112	3.558	233.421	54,486	1.15	11.18	4.85×10^{-2}	.0923	1.18
112	1.109	4.607	301.032	90,621	1.15	11.18	8.09×10^{-2}	.0736	.94
113	1.114	8.681	545.84	297,945	1.15	11.67	2.54×10^{-1}	.0850	1.09
114	1.098	--	--	--	1.15	10.85	--	.0837	1.00
115	1.114	.968	60.865	3,705	1.15	11.67	3.16×10^{-3}	.0890	1.06
116	1.114	4.817	302.882	91,738	1.15	11.67	7.82×10^{-2}	.0890	1.06
117	1.105	7.655	498.871	248,873	1.15	11.18	2.23×10^{-1}	.0734	.88
118	1.114	10.327	649.339	421,642	1.15	11.67	3.59×10^{-1}	.0961	1.15
119	1.121	12.235	774.227	599,428	1.15	11.67	5.07×10^{-1}	.0970	1.16
120	1.194	--	--	--	1.08	11.01	--	.0476	1.00

Table 3 (continued)

Run No.	R	$Q_o x10^{10}$	$qx10^{11}$	q^2x10^{22}	C	U_o	K_I	C_a	E
121	1.212	.410	28.466	810	1.08	11.51	$2.03x10^{-3}$	.0442	.93
122	1.213	1.779	121.817	14,839	1.08	11.67	$3.67x10^{-2}$	.0401	.84
123	1.218	2.623	180.286	32,503	1.08	11.67	$8.02x10^{-2}$	.0363	.76
124	1.197	2.637	180.760	32,674	1.08	11.51	$8.29x10^{-2}$	.0318	.67
125	1.201	4.245	296.321	87,806	1.08	11.34	$2.25x10^{-1}$	.0478	1.00
126	1.190	--	--	--	1.08	12.00	--	.0315	1.00
127	1.169	.505	35.849	1,285	1.08	10.85	$3.55x10^{-3}$	.0427	1.35
128	1.174	2.175	155.042	24,038	1.08	10.85	$6.60x10^{-2}$	.0350	1.11
129	1.157	2.862	207.517	43,063	1.08	10.52	$1.24x10^{-1}$	.0230	.73
130	1.159	2.795	196.903	38,771	1.08	10.85	$1.08x10^{-1}$	.0345	1.10
131	1.161	4.560	331.971	110,205	1.08	10.52	$3.16x10^{-1}$	.0461	1.46
132	1.149	--	--	--	1.08	10.19	--	.0305	1.00
133	1.151	.157	10.354	107	1.08	11.51	$2.83x10^{-4}$	.0343	1.13
134	1.135	.954	64.753	4,193	1.08	11.01	$1.17x10^{-2}$	.0375	1.23
135	1.132	2.575	171.845	29,531	1.08	11.18	$8.16x10^{-2}$	.0450	1.48
136	1.140	2.413	162.219	26,315	1.08	11.18	$7.21x10^{-2}$	.0378	1.24
137	1.153	3.591	233.724	54,627	1.08	11.67	$1.42x10^{-1}$	.0498	1.63
138	1.123	--	--	--	1.08	11.01	--	.0298	1.00
139	1.124	.477	31.618	998	1.08	11.18	$2.78x10^{-3}$	.0298	1.00
140	1.132	1.574	105.041	11,034	1.08	11.18	$3.05x10^{-2}$	.0225	.76

Table 3 (continued)

Run No.	R	$Q_o x10^{10}$	$qx10^{11}$	q^2x10^{22}	C	U_o	K_I	C_a	E
141	1.128	2.637	175.377	30,757	1.08	11.18	$8.56x10^{-2}$	.0223	.75
142	1.133	4.068	267.949	71,797	1.08	11.34	$1.96x10^{-1}$	.0225	.76
143	1.132	4.641	309.722	95,928	1.08	11.18	$2.65x10^{-1}$	.0300	1.01
144	1.209	--	--	--	1.03	11.84	--	.1890	1.00
145	1.192	.286	19.519	381	1.03	11.51	$7.35x10^{-3}$	.1425	.76
146	1.183	1.049	71.028	5,045	1.03	11.51	$9.84x10^{-2}$	.1415	.75
147	1.194	2.113	138.657	19,226	1.03	12.00	$3.57x10^{-1}$	.1191	.63
148	1.194	3.577	234.726	55,096	1.03	12.00	1.02	.1429	.76
149	1.190	3.959	258.543	66,845	1.03	12.00	1.24	.1422	.75
150	1.188	--	--	--	1.03	9.87	--	.1856	1.00
151	1.193	.906	61.024	3,724	1.03	11.67	$7.08x10^{-2}$	.1744	.94
152	1.185	.858	55.834	3,117	1.03	12.00	$5.83x10^{-2}$	.1575	.85
153	1.181	2.270	147.226	21,676	1.03	12.00	$4.07x10^{-1}$	.1530	.82
154	1.190	3.401	222.102	49,329	1.03	12.00	$9.17x10^{-1}$	.1184	.64
155	1.181	2.733	177.256	31,420	1.03	12.00	$5.89x10^{-1}$	.1176	.63
156	1.214	--	--	--	1.03	12.00	--	.1611	1.00
157	1.213	.791	54.163	2,934	1.03	11.67	$5.51x10^{-2}$	.1006	.62
158	1.219	2.590	171.041	29,255	1.03	12.16	$5.24x10^{-1}$	.1337	.83
159	1.209	3.720	243.823	59,450	1.03	12.16	1.07	.1570	.97
160	1.200	5.070	329.677	108,687	1.03	12.16	1.98	.1435	.89

Table 3 (concluded)

Run No.	R	$Q_o x10^{10}$	$qx10^{11}$	q^2x10^{22}	C	U_o	K_I	C_a	E
161	1.200	6.802	442.301	195,630	1.03	12.16	3.56	.0996	.62
162	1.169	--	--	--	1.03	11.51	--	.1165	1.00
163	1.173	1.206	76.609	5,869	1.03	12.16	$1.09x10^{-1}$	.1403	1.20
164	1.169	2.908	132.750	17,623	1.03	12.16	$3.29x10^{-1}$	.2056	1.77
165	1.177	3.463	220.885	48,790	1.03	12.16	$9.03x10^{-1}$	.2190	1.88
166	1.183	3.510	219.132	48,019	1.03	12.49	$8.63x10^{-1}$	.1729	1.48
167	1.175	5.929	367.258	134,879	1.03	12.49	2.44	.1521	1.31

Table 4. Supplementary Calculated Parameters

Run No.	R	C_p	Run No.	R	C_p
1	1.139	3.42×10^{7}	31	1.155	3.86×10^{5}
2	1.146	2.68×10^{7}	32	1.138	1.52×10^{6}
3	1.225	2.06×10^{7}	33	1.121	2.06×10^{6}
4	1.111	2.41×10^{7}	34	1.136	2.09×10^{6}
5	1.082	1.45×10^{7}	35	1.132	1.32×10^{6}
6	1.109	2.61×10^{7}	36	1.153	0.0
7	1.109	2.59×10^{7}	37	1.147	3.84×10^{5}
8	1.094	1.46×10^{7}	38	1.185	1.38×10^{6}
9	1.075	7.23×10^{6}	39	1.185	1.59×10^{6}
10	1.080	1.80×10^{7}	40	1.196	2.19×10^{6}
11	1.094	1.46×10^{7}	41	1.176	2.60×10^{6}
12	1.070	1.09×10^{7}	42	1.129	3.78×10^{5}
13	1.105	1.11×10^{7}	43	1.117	1.31×10^{6}
14	1.087	9.08×10^{6}	44	1.150	2.11×10^{6}
15	1.087	1.09×10^{7}	45	1.136	2.85×10^{6}
16	1.084	1.45×10^{7}	46	1.094	3.11×10^{6}
17	1.076	7.20×10^{6}	47	1.112	3.72×10^{6}
18	1.105	1.48×10^{7}	48	1.135	6.83×10^{5}
19	1.101	1.10×10^{7}	49	1.155	6.57×10^{5}
20	1.109	1.48×10^{7}	50	1.131	6.04×10^{5}
21	1.087	1.09×10^{7}	51	1.131	4.91×10^{5}
22	1.075	1.08×10^{7}	52	1.136	6.84×10^{5}
23	1.064	1.07×10^{7}	53	1.118	3.74×10^{5}
24	1.093	0.0	54	1.118	6.74×10^{5}
25	1.142	1.91×10^{5}	55	1.123	6.00×10^{5}
26	1.138	0.0	56	1.124	3.76×10^{5}
27	1.139	0.0	57	1.151	5.0×10^{5}
28	1.121	1.31×10^{6}	58	1.133	3.79×10^{5}
29	1.129	2.08×10^{6}	59	1.159	6.19×10^{5}
30	1.146	0.0	60	1.110	4.83×10^{5}

Table 4 (continued)

Run No.	R	C_p	Run No.	R	C_p
61	1.117	6.72×10^5	91	1.143	1.53×10^5
62	1.152	5.00×10^5	92	1.155	1.55×10^5
63	1.153	3.85×10^5	93	1.129	1.79×10^5
64	1.153	3.85×10^5	94	1.183	2.28×10^5
65	1.140	3.81×10^5	95	1.138	2.56×10^5
66	1.135	3.79×10^5	96	1.144	1.53×10^5
67	1.146	4.98×10^5	97	1.118	1.01×10^5
68	1.144	6.13×10^5	98	1.124	8.64×10^4
69	1.124	3.76×10^5	99	1.101	1.55×10^5
70	1.142	5.34×10^5	100	1.107	8.51×10^4
71	1.120	5.24×10^5	101	1.128	1.51×10^5
72	1.129	2.17×10^5	102	1.124	1.16×10^5
73	1.164	1.56×10^5	103	1.129	1.17×10^5
74	1.153	2.23×10^5	104	1.099	1.47×10^5
75	1.164	1.85×10^5	105	1.127	1.50×10^5
76	1.142	2.19×10^5	106	1.114	1.60×10^5
77	1.138	1.52×10^5	107	1.144	1.03×10^5
78	1.153	1.54×10^5	108	1.116	1.23×10^5
79	1.155	2.22×10^5	109	1.114	1.00×10^5
80	1.182	2.07×10^5	110	1.116	1.01×10^5
81	1.157	1.55×10^5	111	1.112	1.49×10^5
82	1.171	1.86×10^5	112	1.109	1.15×10^5
83	1.157	2.61×10^5	113	1.114	1.34×10^5
84	1.127	1.79×10^5	114	1.098	1.32×10^5
85	1.109	1.94×10^5	115	1.114	1.41×10^5
86	1.131	1.80×10^5	116	1.114	1.41×10^5
87	1.155	1.55×10^5	117	1.105	1.14×10^5
88	1.151	2.02×10^5	118	1.114	1.49×10^5
89	1.143	1.81×10^5	119	1.121	1.50×10^5
90	1.155	1.84×10^5	120	1.194	1.10×10^5

Table 4 (concluded)

Run No.	R	C_p	Run No.	R	C_p
121	1.212	1.05×10^5	146	1.183	1.46×10^4
122	1.213	1.01×10^5	147	1.194	1.20×10^4
123	1.218	8.54×10^4	148	1.194	1.48×10^4
124	1.197	8.00×10^4	149	1.190	1.19×10^4
125	1.201	1.08×10^5	150	1.188	1.99×10^4
126	1.190	7.95×10^4	151	1.193	1.87×10^4
127	1.169	1.02×10^5	152	1.185	1.70×10^4
128	1.174	8.23×10^4	153	1.181	1.58×10^4
129	1.157	6.19×10^4	154	1.190	1.19×10^4
130	1.159	8.15×10^4	155	1.181	1.18×10^4
131	1.161	1.05×10^5	156	1.214	1.74×10^4
132	1.149	7.30×10^4	157	1.213	9.72×10^3
133	1.151	8.09×10^4	158	1.219	1.35×10^4
134	1.135	9.48×10^4	159	1.209	1.62×10^4
135	1.132	1.02×10^5	160	1.200	1.48×10^4
136	1.140	9.53×10^4	161	1.200	9.62×10^3
137	1.153	1.19×10^5	162	1.169	1.17×10^4
138	1.123	7.12×10^4	163	1.173	1.45×10^4
139	1.124	7.14×10^4	164	1.169	2.19×10^4
140	1.132	6.05×10^4	165	1.177	2.28×10^4
141	1.128	6.03×10^4	166	1.183	1.82×10^4
142	1.133	6.07×10^4	167	1.175	1.57×10^4
143	1.132	7.19×10^4			
144	1.209	2.02×10^4			
145	1.192	1.47×10^4			

BIBLIOGRAPHY

1. Fuchs, N. A., The Mechanics of Aerosols, Pergamon Press, Inc., New York, New York (1964).

2. Davies, C. N., (edited), Aerosol Science, Academic Press, New York, New York (1966).

3. Green, H. L. and Lane, W. R., Particulate Clouds: Dusts, Smokes, and Mists, 2nd Ed., D. Van Nostrand Company, Inc., Princeton, New Jersey (1964).

4. Wilson, I. B., quoted in (2), pp. 78.

5. Davies, C. N., quoted in (1), pp. 173.

6. Fuchs, N. A. and others, "On the Determination of Particle Size Distribution in Polydisperse Aerosols by the Diffusion Method," Brit. J. Appl. Phys., 1962, 13, 280.

7. Zebel, G., "Deposition of Aerosol Flowing Past a Cylindral Fiber in a Uniform Electric Field," J. Coll. Sci., 1965, 20, 522.

8. Natanson, G. L., quoted in (2), pp. 75.

9. Walton, W. H. and Woolcock, A., "The Suppression of Airborne Dust by Water Spray," Int. J. Air Poll., 1960, 3, 129.

10. Picknett, R. G., "Collection Efficiencies for Water Drops in Air," Int. J. Air Poll., 1960, 3, 160.

11. Khimach, M. and Shishkin, N., quoted in (1), pp. 167.

12. Pemberton, C. S., "Scavenging Action of Rain on Non-Wettable Particulate Matter Suspended in the Atmosphere," Int. J. Air Poll., 1960, 3, 165.

13. Oakes, B., "Laboratory Experiments Relating to the Wash-out of Particles by Rain," Int. J. Air Poll., 1960, 3, 179.

14. Herne, H. and Fonda, G., "The Classical Computations of the Aerodynamic Capture of Particles by Spheres," Int. J. Air Poll., 1960, 3, 26.

15. Lundgren, D. A. and Whitby, K. T., qucted in (2), pp. 75.

16. Gillespie, T., "Electric Charge Effects in Aerosol Collosion Phenomena," Int. J. Air Poll., 1960, 3, 44.

17. Gunn, K. and Hitschfeld, W., "A Laboratory Investigation of the Coalescence Between Large and Small Water Drops," J. Meteor., 1951, 8, 7.

18. Kraemer, H. and Johnstone, H., "Collection of Aerosol Particles in Presence of Electric Fields," Ind. Eng. Chem., 1955, 47, 2426.

19. Matteson, M. J. and Giardina, P. J., "Mass Transfer of Sulfur Dioxide to Growing Droplets," Environmental Science and Technology, 1974, 8, 50.

20. Lewis, L., "The Collection of Aerosol Particles by Charged Water Droplets," Master's Thesis in Physics, Georgia Institute of Technology, 1973.

21. Pilat, M. J., Jaasund, S. A., and Sparks, L. E., "Collection of Aerosol Particles by Electrostatic Droplet Spray Scrubbers," Environmental Science and Technology, 1974, 8, 360.

22. Liu, Benjamin Y. H. and Pui, David Y. H., "Electrical Neutralization of Aerosols," Particle Technology Laboratory Publication No. 223, University of Minnesota, 1974.

23. Mercer, Thomas T., Aerosol Technology in Hazard Evaluation, Academic Press, New York, New York (1973), pp. 28.

24. Beers, Y., Theory of Error, Addison-Wesley Publishing Company, Cambridge, Massachusetts (1953), pp. 34.